LA-UR-18-29048
Approved for public release; distribution is unlimited.

Title: QED: A different perspective

Author(s): Lestone, John Paul

Intended for: To be submitted to the Journal of Modern Physics

Issued: 2018-09-24

LA-UR-18-xxxxx

QED: A different perspective

J. P. Lestone
Computational Physics Division, Los Alamos National Laboratory
Los Alamos, NM 87545, USA
September 20th, 2018

Abstract

A simple picture of the electron emerges by invoking a cross section of $\pi\lambda\!\!\!^{-2}$ for vacuum virtual photons to stimulate an isolated electron to emit an additional virtual photon. This reaction mechanism leads to the storage of the rest energy in the surrounding cloud of stimulated virtual photons. Inertia appears to be associated with the Doppler shift of self-absorbed stimulated virtual photons. The Lamb shift can be obtained if one out of every $1/\alpha$ of the stimulated emissions is preceded by the absorption and re-emission of the incident vacuum virtual photon including the corresponding electron recoil. This suggests a "doorway" cross section of $\alpha\pi\lambda\!\!\!^{-2}$ plays a role in some QED processes. This is supported by a semi-classical picture of Compton scattering. Several semi-classical reaction mechanism choices, including near-field effects, give the anomalous magnetic moment of the free electron, and the magnetic moment of electrons in hydrogen-like atoms close to the correct result. Stimulated-emission and reabsorption processes allow for virtual photons to be exchanged between an electron pair. This exchange can be used to estimate a repulsive force between electrons, and thus the fine-structure constant. Simple assumptions can be made that suggest a fraction of the exchanging virtual-photon energy is scattered to infinity, with an emission power close to the Larmor formula. Conservation of energy can be maintained without invoking the electromagnetic force of an electron on itself. In the presented model charge is an emergent property of the whole electron, with no mechanism by which the electron can be subdivided into smaller self-interacting pieces.

I. Introduction

Quantum electrodynamics (QED) is one of the most successful and tested theories ever developed, and can be viewed as a pinnacle of human thought. QED's development was not easy and it took several decades of concerted effort by many authors to obtain a working theory capable of giving precise predictions. The first steps to a usable theory of the interaction of matter and light, consistent with both special relativity and quantum mechanics, were taken by Dirac in the late 1920s [DIR27]. Significant contributions by others followed, culminating in a series of papers by Tomonaga [TOM46], Schwinger [SCH48], Feynman [FEY49], and Dyson [DYS49]. Those trained in QED have since been able to calculate many experimental observables with extraordinary precision. However, precise manual calculations require monumental effort, and are not amenable to a lone physicist with a casual interest in QED. For example, the anomalous magnetic moment of the electron, $(g-2)/2$, was not obtained to fourth- and sixth-order until 1957 [PET57] and 1996 [LAP96], respectively. The theoretical relationship between $(g-2)/2$ and the fine-structure constant, α, is now known to tenth order [KIN06, AOY07, AOY12], and considered to be so strong, and the modern $(g-2)/2$ measurements so precise [GAB06],

that the modern estimate of α = 1/137.0359991 [MOH15] is inferred from (g–2)/2 measurements via QED theory.

Unfortunately, a full and detailed understanding of QED requires both talent and a significant time commitment. The aim of the present study is to find a series of relatively simple semi-classical assumptions and/or reaction mechanisms that can be used to calculate several QED based phenomena without the use of full quantum theory or detailed special relativity. We will not necessarily attempt a detailed justification of all the assumptions, but note that thinking a certain way leads to computational results that are close to experimental observations. Many of these assumptions will appear unorthodox to those who are experts in QED, but perhaps resonate with those looking for a simple way of obtaining a more intuitive feel of some QED processes without the investment in time required to obtain a full understanding. A guiding principle used here, is the hope that most physics is simple. This hope is not necessarily a recipe for success. Be aware that the simple semi-classical reaction mechanisms presented here are reverse-engineered from the known experimental results, and are no substitute for standard quantum field theory calculations. However, the approaches used here to obtain simple methods for a partial understanding of some QED processes do lead to a possible explanation for the numerical value of the fine-structure constant.

II. Vacuum virtual photon electron interaction cross section

The main theme of this manuscript is the consideration that there is a fundamental photon-electron interaction cross section at the heart of QED processes. The size and the consequences of this cross section can be examined by calculating observable outcomes from various hypotheses, and comparing to the corresponding experimental results.

The interaction cross section between spherically symmetric projectiles and targets can be written as

$$\sigma(\varepsilon) = \sum_{L=0}^{\infty} T_L(\varepsilon)\pi\lambda\!\!\!^{-2}, \qquad \text{(II. 1)}$$

where $\lambda\!\!\!^{-}$ is the reduced wavelength of the projectile-target system, and the $T_L(\varepsilon)$ are orbital angular momentum and energy-dependent transmission coefficients. In the limit of very small point-like objects (without long-range forces) an interaction can only proceed via central collisions with no relative orbital angular momentum. This is why low-energy neutron-induced reactions proceed via the L=0 incoming s wave. For the photon-electron interaction, our first assumption is: $T_{L=0}(\varepsilon)$ = 1 for ε less than a high-energy cutoff ε_H, and zero for all $L\neq0$; i.e. an interaction cross section of $\pi\lambda\!\!\!^{-2}$ for $\varepsilon < \varepsilon_H$. The consequence associated with this cross section is our second assumption: the electron is stimulated to emit an additional virtual photon (a stimulated virtual photon), while the incident vacuum virtual photon proceeds on as if nothing has happened. The direction of the simulated emission is not the same as the incident photon, because the effective size of the emitter is small. This is analogous to the Hanbury Brown and Twiss effect [HAN56] where correlated photons emitted from an object are not emitted parallel, but with typical angles between the correlated photons of ~ $\lambda\!\!\!^{-}$ divided by the radius of the emitter. Here, the effective size of the emitter is small, and we assume the stimulated photons are emitted uniformly into 4π. The stimulated emission of a virtual photon by the passage of the nearby vacuum virtual photon is depicted in Fig. II.1 (and later in Fig. II.2).

The stimulated emission from a fixed-mass object, like an electron, violates conservation of energy and momentum, and would not be allowed if only classical physics was assumed. We invoke the time-energy uncertainty principle and allow the stimulated emission to travel away from the electron at the speed of light c and "disappear" on a time scale of $\hbar/(2\varepsilon)$. This gives an exponential distribution of the

semi-classical survival times, $P(t) \propto \exp(-2t\varepsilon/\hbar)$, with the stimulated virtual photons travelling approximately one-half their reduced wave length before "disappearing." This will be modified later with the addition of self-absorption, reabsorption, and the absorption by a neighboring particle as other methods by which the stimulated photon can end its life.

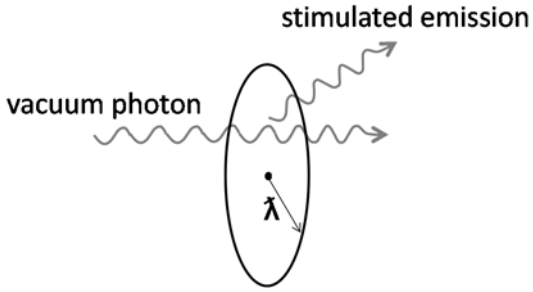

Fig. II.1. Depiction of a stimulated virtual emission generated by the passage of the vacuum virtual photon within ƛ of a point particle. The wavelength of the schematic photons is not to scale.

The high-energy cutoff, ε_H, can be estimated via a variety of thought experiments. Thinking semi-classically, photons can interact fully with (i.e. shake) an isolated electron when the wavelength is much larger than an electron's effective size. If the wavelength of an incident electromagnetic wave becomes smaller than an electron's effective size then different parts of the high-frequency wave "try" to push different parts of the electron in opposite directions, and thus the overall strength of the total interaction (shaking) decreases. Setting the wavelength of the high-energy cutoff to the reduced Compton wavelength $ƛ_C = \hbar c/(mc^2)$ gives $\varepsilon_H \sim hc/ƛ_C = 2\pi mc^2$. This logic is relatively vague, and should not be believed unless backed up by additional arguments (see below).

II.A Virtual-photon emission rate from an electron

The stimulated-emission rate from an isolated electron can be determined by multiplying the production cross section by the number density of vacuum virtual photons [BJO64] by the speed of light

$$R = \int_0^{\varepsilon_H} R(\varepsilon)d\varepsilon = \int_0^{\varepsilon_H} \pi ƛ^2 \frac{\varepsilon^2 d\varepsilon}{\pi^2\hbar^3c^3} c = \int_0^{\varepsilon_H} \frac{d\varepsilon}{\pi\hbar} = \frac{\varepsilon_H}{\pi\hbar}\,. \qquad \text{(II.2)}$$

We have assumed ε_H operates as a sharp cutoff. This sharp cutoff is likely unphysical. However, we apply the philosophy that if a simplistic approach appears to be adequate then we keep it until a more sophisticated one is needed. All spontaneous-photon emission rates can be viewed as stimulated emission induced by vacuum virtual photons, and thus Eq. (II.2) can be viewed as the spontaneous-emission rate of virtual photons from an electron.

II.B Rest energy of the electron

Combining Eq. (II.2) with the time-energy uncertainty principle, the additional average virtual-photon energy (above the virtual-photon vacuum ground-state energy) associated with the presence of an isolated electron can be expressed as

$$\begin{aligned}\bar{E} &= \int_0^{\varepsilon_H}\int_0^{\infty} \frac{\varepsilon}{\pi\hbar}\frac{t\exp(-2\varepsilon t/\hbar)\,dt}{\int_0^{\infty}\exp(-2\varepsilon t/\hbar)\,dt}d\varepsilon \\ &= \int_0^{\varepsilon_H}\int_0^{\infty} \frac{2\varepsilon^2}{\pi\hbar^2} t\exp(-2\varepsilon t/\hbar)\,dt\,d\varepsilon = \frac{1}{2\pi}\int_0^{\varepsilon_H} d\varepsilon = \frac{\varepsilon_H}{2\pi} = mc^2. \qquad \text{(II.3)}\end{aligned}$$

This result supports the previous suggestion that the high-energy cutoff is $\varepsilon_H = 2\pi mc^2$. The reaction mechanism by which Eq. (II.3) gives the rest energy is pictured in Fig. II.2.

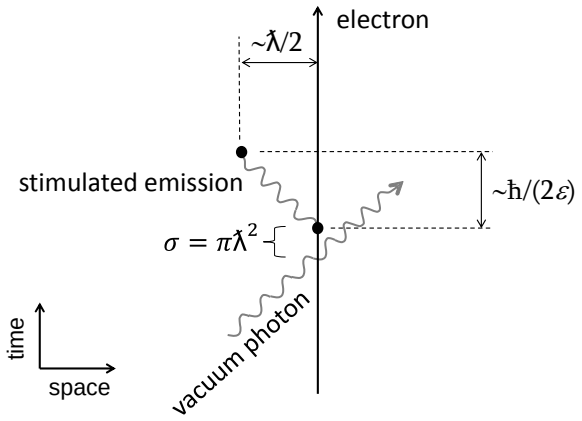

Fig. II.2. A Feynman-like diagram of the proposed mechanism by which the rest energy of an electron is stored in the surrounding cloud of stimulated virtual photons generated by an interaction of the "naked" electron with the vacuum virtual photons.

This mechanism does not explain the size of the electron's mass, but does give a physical mechanism for the existence of the rest energy as the energy tied up in the cloud of stimulated virtual photons surrounding an isolated electron. With this explanation, one could assume that the high-energy cutoff is the fundamental quantity, and this leads to a particle's rest energy equal to the reduced cutoff energy which, in turn, leads to an effective size consistent with the assumed cutoff. This interpretation has no problem with point-like particles, unlike the storage of the rest energy in the electric field surrounding a classical point particle. The concept of an electron's energy being contained in a surrounding cloud of virtual photons gives the relativistic mass of a particle as a function of its velocity, because of the different rates of the passage of time between different inertial frames that control the time-energy uncertainty principle. The Doppler shift of the virtual photons associated with a particle's velocity gives the result that a particle's momentum is stored in the surrounding cloud of virtual photons (a simple exercise for the reader).

A semi-classical picture of why charged particles can "erupt" from the vacuum for a short time period is also obtained. This is because of the interpretation that the rest energy is stored in the surrounding cloud of stimulated virtual photons, and not in the point-like particle in the middle of the cloud. If a naked point-like particle is born at time t=0 (without its cloud of stimulated virtual photons) it will take a finite time scale for the first vacuum virtual photon to find the new particle. This time scale is the inverse of the rate given by Eq (II.2) and is equal to $\pi\hbar/\varepsilon_H = \hbar/(2mc^2)$, in agreement with the time-energy uncertainty principle. This is not surprising, because the time-energy uncertainty principle is one of the inputted assumptions. What is of interest is that a simple semi-classical picture emerges, and that this picture is only self-consistent with the time-energy uncertainty principle if the high-energy cutoff is $\varepsilon_H = 2\pi mc^2$.

The results obtained thus far suggest that a naked electron has no intrinsic mass; the energy of the whole electron is defined by a finite high-energy cutoff ($\varepsilon_H=2\pi mc^2$ where m is the electron's mass) in the photon naked-electron cross section; the average energy stored in the surrounding cloud of stimulated virtual photons is mc^2; and it takes a time scale of $\hbar/(2mc^2)$ after the birth of a naked electron for a vacuum virtual photon to find the electron and generate the first rest-energy (mass) storing stimulated virtual photon.

II.C Inertia

The rest-energy storage mechanism introduced above gives the correct particle energy as a function of velocity and thus also the correct inertia. However, it is of interest to consider what microscopic processes are causing this inertia. We imagine the emitted stimulated virtual photons are self-absorbed after a time period of ~ħ/ε. If during this time an electron is accelerated by an external force, the stimulated virtual photons responsible for the rest energy will "return" Doppler shifted as seen by the electron. Virtual photons emitted in the direction of the acceleration will be returned Doppler shifted to a higher frequency (and thus higher momentum) and will thus resist the external force. Similarly, virtual photons emitted opposite to the external force will be Doppler shifted to a lower momentum on their return and also oppose the external force. Averaging over a long enough time period, an electron cannot recoil from a small impulse at the speed of light but instead recoil with a smaller speed controlled by the high-energy cutoff, $\varepsilon_H = 2\pi mc^2$.

As stated in the introduction, we here reverse-engineer semi-classical "explanations" to give the desired results, instead of using first-principle derivations starting from a solid theoretical foundation. The correct inertia can be obtained if we assume the stimulated virtual emission and self-absorption process is divided into four steps: (1) emission; (2) free flight away; (3) return flight; and (4) self-absorption, with each of these steps taking a time scale of ħ/(2ε). To keep section II.B unchanged, only the photon's free flight away contributes to the rest energy of a particle. The effective times for emission and self-absorption are set to be halfway through the respective emission and self-absorption time periods (see Fig. II.3). The average time between the effective emission and self-absorption for the calculation of the Doppler shifts associated with particle acceleration is then $\tau_{e\to s}$=3ħ/(2ε).

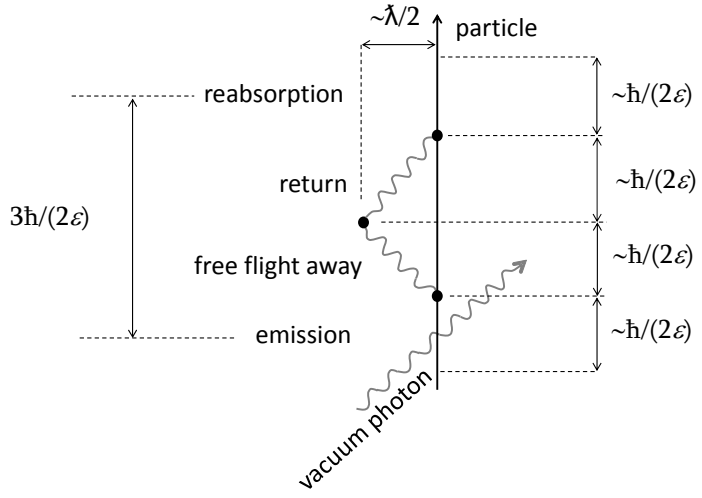

Fig. II.3. An update to the Feynman-like diagram presented in Fig. II.2 to give inertia.

If an electron has an acceleration a, then its speed change between the effective emission and self-absorption times is $\Delta v = 3a\hbar/(2\varepsilon)$. The corresponding momentum change per unit time associated with the emission and self-absorption of the virtual photons responsible for a particle's rest energy is given by

$$\frac{dP}{dt} = \int_0^{\pi}\int_0^{\varepsilon_H} \frac{\varepsilon\cos(\theta)}{c}\frac{d\varepsilon}{\pi\hbar}\left(\frac{\Delta v}{c}\cos(\theta)\right)\frac{\sin(\theta)d\theta}{2}$$

$$= \frac{1}{2\pi\hbar c}\int_0^{\pi}\int_0^{\varepsilon_H}\left(\frac{3a\hbar}{2c}\cos^2(\theta)\sin(\theta)\right)d\varepsilon\, d\theta$$
$$= \frac{3a\varepsilon_H}{4\pi c^2}\int_0^{\pi}\cos^2(\theta)\sin(\theta)\; d\theta = \frac{a\varepsilon_H}{2\pi c^2} = ma, \qquad \text{(II. 4)}$$

where θ is the angle of emission relative to the direction of the external force. Therefore, when an external force F is applied to a particle with a non-zero high-energy cutoff $\varepsilon_H = 2\pi mc^2$, the emission and self-absorption of the virtual photons limit the electron's acceleration to $a=F/m$, on time scales longer than $\pi\hbar/\varepsilon_H = \hbar/(2mc^2)$. On shorter time scales much higher accelerations are possible with "instantaneous" speeds only limited by the speed of light.

II.D Black-body emission

The spontaneous photon emission rate from a spherical black-body can be obtained via transition state theory, with an emission rate from a large black-body sphere (excluding stimulated emissions in the black-body's surface) [LES08]

$$R = \frac{2}{2\pi\hbar}\int_0^{\infty}\sum_{L=0}^{L_{\max}}(2L+1)\exp(-\varepsilon/T)\, d\varepsilon. \qquad \text{(II. 5)}$$

The maximum angular momentum that a photon can carry away from a macroscopic sphere of radius r is $L_{max}\hbar = r\varepsilon/c$. Substituting into Eq. (II.5), and taking the limit of a large macroscopic object, gives the spontaneous emission rate [LES08]

$$R = \frac{4\pi r^2}{4\pi^2\hbar^3c^2}\int_0^{\infty}\varepsilon^2\exp(-\varepsilon/T)\, d\varepsilon. \qquad \text{(II. 6)}$$

In the limit of a very small object, only L=0 emission is allowed, and the spontaneous-emission rate becomes

$$R = \frac{1}{\pi\hbar}\int_0^{\infty}\exp(-\varepsilon/T)\, d\varepsilon. \qquad \text{(II. 7)}$$

In the limit of an infinitely hot object, this rate becomes

$$R = \frac{1}{\pi\hbar}\int_0^{\varepsilon_H} d\varepsilon = \frac{\varepsilon_H}{\pi\hbar}. \qquad \text{(II. 8)}$$

This result is the same as Eq. (II.2), and suggests the above-discussed assumptions are the same as assuming electrons behave like very small and very hot black bodies. This suggests electrons resemble virtual-photon Hawking-radiating micro black holes.

The emission represented by Eq. (II.8) violates conservation of energy and momentum if from a fixed-mass object like an electron, and would not be allowed if only classical physics was assumed. However, in a time scale of ~$\hbar/(2\varepsilon)$ some of the stimulated virtual photon can re-establish the appropriate conservation rules by being absorbed by a nearby partner electron, thus enabling the exchange of virtual photons between two electrons. The rest of this manuscript provides support that this exchange mechanism is the cause of the electromagnetic repulsion between two electrons. This force can be used to estimate the numerical value of the fine-structure constant. Before estimating the fine-structure constant, we determine other details that appear important to a semi-classical understanding of virtual-photon electron interactions by studying the Lamb shift, Compton scattering, and the magnetic moment of electrons in the next three sections.

III. Hydrogen Lamb shift

According to the Dirac equation, the hydrogen $2s_{1/2}$ and $2p_{1/2}$ levels are degenerate. This is a consequence of an assumed pure inverse-square-law Coulomb force between the electron and the proton. There are many reasons why the true interaction is not a perfect inverse-square law at small distances. These include the finite size of the proton, vacuum polarization associated with virtual electron-positron pairs [UEH35], and a possible intrinsic fuzziness of the electromagnetic interaction involving electrons on small length scales. In 1947 Lamb and Retherford [LAM47] demonstrated that the hydrogen $2s_{1/2}$ level sits ~1000 MHz above the $2p_{1/2}$ level. Bethe showed in the same year [BET47] that this observation was predominantly due to the electromagnetic vacuum interacting with the electron. A more modern measurement of the Lamb shift is 1057.85 MHz and is consistent with QED calculations [KAR98].

Welton [WEL48, BJO64] obtained a qualitative description of the Lamb shift, by invoking a semi-classical model of the time dependence of the electric field of the vacuum state, and how these fluctuations smear out the location of an electron. The corresponding root-mean-square (rms) spread in the electron's location associated with its interaction with the vacuum is [BJO64, pg. 60]

$$\delta r^2 = \frac{2\alpha \lambda\!\!\!^{-2}_{C}}{\pi} \int \frac{d\varepsilon}{\varepsilon}. \tag{III. 1}$$

To obtain a finite result, there need to be both low- and high-energy cutoffs. A possible value for the high-energy cutoff is discussed above ($\varepsilon_H = 2\pi mc^2$). For a bound electron, there must be a low-energy cutoff, because wavelengths larger than the characteristic size of the system (approximately the Bohr radius) cannot see the electron and proton as independent objects. We assume the Lamb shift low-energy cutoff is the energy of a photon with a wavelength equal to one-half the Bohr circumference, i.e. the distance travelled by the electron to get to the opposite side of the atom (assuming a circular path). This gives $\varepsilon_L = \alpha mc^2/\pi$.

From the Darwin term in the Dirac equation it follows that the hydrogen Lamb shift is [BJO64, pg. 59]

$$\Delta E_n = \frac{2\pi}{3} \alpha \hbar c \; \delta r^2 \; |\psi_n(0)|^2. \tag{III. 2}$$

For those not familiar with the Dirac equation, this is not very transparent, so we also show a derivation of Eq. (III.2) using first-order perturbation theory where the shift in the energy of a given state is

$$\Delta E = \int \psi \, \Delta V \, \psi^* dv \,, \tag{III. 3}$$

where ΔV is the perturbation of the potential. Invoking the large number of randomly orientated and phased vacuum modes and the central-limit theorem, the blurriness of an electron's charge associated with its interaction with the electromagnetic vacuum will be Gaussian with a variance of δr^2 [see Eq. (III.1)]. The size of the Lamb shift can be shown to depend only on the rms spread of the electron's blurriness, and not on the details of the shape of the distribution (an exercise for the reader). Given this, we choose the simplest charge distribution of a delta spike at a radius of δr to evaluate the Lamb shift. This choice causes ΔV to be zero for $r > \delta r$ and $\Delta V = \alpha\hbar c(1/r - 1/\delta r)$ for $r < \delta r$, and enables us to write the shift in a hydrogen level as

$$\Delta E = \int_0^{\delta r} |\psi(r)|^2 \alpha \hbar c \left(\frac{1}{r} - \frac{1}{\delta r}\right) 4\pi r^2 \, dr. \tag{III. 4}$$

Given that $\delta r << \lambda\!\!\!^{-}_{C}/\alpha$, the radial dependences of the *s* wave function can be set constant over the range of the integral in Eq. (III.4) giving

$$\Delta E_{ns} = 4\pi\alpha\hbar c|\psi_{ns}(0)|^2 \int_0^{\delta r}\left(r - \frac{r^2}{\delta r}\right) dr = \frac{2\pi}{3}\alpha\hbar c\, \delta r^2\, |\psi_{ns}(0)|^2, \qquad \text{(III. 5)}$$

in agreement with Eq. (III.2).

If we apply the low- and high-energy cutoffs of $\alpha mc^2/\pi$ and $2\pi mc^2$ to Eq. (III.1) then

$$\delta r^2 = \frac{2\alpha\lambda\!\!\!^{-2}_{\rm C}}{\pi}\int_{\alpha/\pi}^{2\pi}\frac{d\varepsilon}{\varepsilon} = \frac{2\alpha\,\ln(2\pi^2/\alpha)\lambda\!\!\!^{-2}_{\rm C}}{\pi} \quad \text{and} \quad \Delta E_{2s} = \frac{\alpha^5\,\ln(2\pi^2/\alpha)}{6\pi}\,mc^2 = 1072\text{ MHz}. \qquad \text{(III. 6)}$$

Correcting for the shift in the $2s$ level associated with the polarization of the vacuum [UEH35] (–27 MHz), the shift in the $2p_{1/2}$ level [BET50, KAR52] by −13 MHz, and the small correction due to the proton's size [KEM33] (<0.2 MHz) gives a final estimate of the hydrogen Lamb shift of 1058 MHz. Given the approximations made, the level of agreement with experiment is stunning, but possibly fortuitous. The success of Eq. (III.6) may be due to a more prudent choice of cutoff energies, and the fact that simple semi-classical methods sometimes give accurate results as demonstrated by the Bohr theory of the hydrogen atom.

We now introduce a new method for obtaining Eq. (III.1) by invoking a semi-classical photon-based picture of the electromagnetic vacuum. We assume that stimulated emission is not the only consequence of the $\pi\lambda\!\!\!^{-2}$ interaction cross section introduced in section II and invoke: one out of every $1/\alpha$ of the stimulated emissions involves the initial absorption of the incident photon, the recoil of the electron, and then the re-emission of the original photon. The initial absorption violates conservation of energy and momentum and would not be allowed if only classical physics was assumed. We invoke the time-energy uncertainty principle to allow the absorption to occur, as long as the absorbed photon is re-emitted on a time scale of $\tau \sim \hbar/\varepsilon$ (see Fig. III.1). We have allowed a time scale of ~$\hbar/(2\varepsilon)$ for each of the absorption and emission processes. Given these assumptions, the rate that vacuum virtual photons are absorbed (and then re-emitted) by an isolated electron can be obtained by multiplying Eq. (II.2) by α, giving

$$R_{\rm a}(\varepsilon) = \alpha\pi\lambda\!\!\!^{-2}\frac{\varepsilon^2 d\varepsilon}{\pi^2\hbar^3c^3}c = \frac{\alpha d\varepsilon}{\pi\hbar}. \qquad \text{(III. 7)}$$

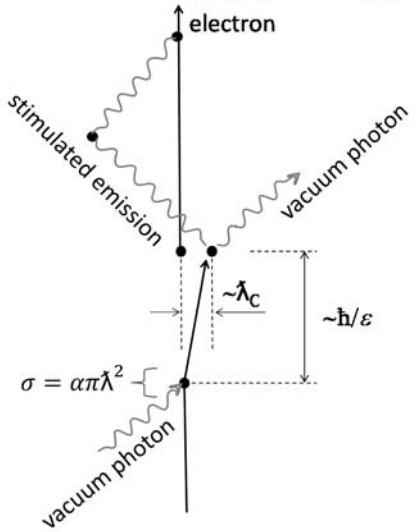

Fig. III.1. A Feynman-like diagram of the reaction mechanism used to obtain Eq. (III.8) (the Lamb shift). This diagram is the same as in Fig. II.3, except the incident vacuum virtual photon is first absorbed with a cross section of $\alpha\pi\lambda\!\!\!^{-2}$ and then re-emitted. The additional stimulated virtual photon is emitted at the same time. To keep the total interaction cross section of $\pi\lambda\!\!\!^{-2}$, the recoil-less reaction cross section (see Fig. II.2) is reduced to $(1-\alpha)\pi\lambda\!\!\!^{-2}$.

On absorption (in the non-relativistic limit), the electron recoils with a velocity of $\varepsilon/(mc)$ and travels a distance $r \sim \varepsilon/(mc)\times\hbar/\varepsilon = \lambda\!\!\!^{-}_C$, before the absorbed photon is re-emitted. The emission of the additional stimulated photon is assumed to occur at this time. Following the re-emission and stimulated emission we assume the electron is instantaneously returned to its original pre-absorbed state. A Feynman-like diagram depicting these assumptions is presented in Fig. III.1. If the probability per unit time to complete the combined absorption and re-emission process is assumed to be $\hbar/\varepsilon$, then there will be an exponential ensemble of recoil distances, $\exp(-r/\lambda\!\!\!^{-}_C)$, with a mean value of $\lambda\!\!\!^{-}_C$. The same result is obtained with relativistic kinetics if the time scale $\tau = \hbar/\varepsilon$ is assumed to apply in the reference frame of the recoiling particle. For a given recoil distance r, the rms spread of the electron's location averaged along its path is $r^2/3$ (assuming a constant recoil velocity), with a recoil time of rmc/ε. Combining these effects gives an rms spread of an electron's location due to the recoils associated with the absorption and re-emission of vacuum virtual photons of

$$\delta r^2(\varepsilon) = \frac{\int_0^\infty \frac{r^2}{3}\frac{rmc}{\varepsilon}\frac{\alpha d\varepsilon}{\pi\hbar}\exp(-r/\lambda\!\!\!^{-}_C)dr}{\int_0^\infty \exp(-r/\lambda\!\!\!^{-}_C)dr} = \frac{\alpha mc^2}{3\lambda\!\!\!^{-}_C\pi\hbar c}\frac{d\varepsilon}{\varepsilon}\int_0^\infty r^3\exp\left(-\frac{r}{\lambda\!\!\!^{-}_C}\right)dr = \frac{2\alpha\lambda\!\!\!^{-2}_C}{\pi}\frac{d\varepsilon}{\varepsilon}. \quad \text{(III.8)}$$

Integrating Eq. (III.8) over the energy of the relevant vacuum photons gives Eq. (III.1). This result partially justifies the assumed $\alpha\pi\lambda\!\!\!^{-2}$ vacuum-virtual-photon absorption cross section. The apparent success in obtaining a simple method by which the Lamb shift can be understood, suggests that a "doorway" cross section of $\alpha\pi\lambda\!\!\!^{-2}$ plays a role in some QED processes. To test this hypothesis, we attempt to obtain a simple understanding of Compton scattering in the next section.

IV. Compton scattering

The $\alpha\pi\lambda\!\!\!^{-2}$ vacuum-virtual-photon absorption cross section used in section III can be thought of as a first step (a doorway cross section) in the process of Compton scattering. First, the electron makes an attempt to absorb the incident real photon with a cross section $\alpha\pi\lambda\!\!\!^{-2}$. If no other steps occur, this attempted absorption must fail as in section III, with the re-emission of the incident photon. In the second step, the electron is assumed to recoil with velocity $v = \varepsilon/(mc)$, which it obtains over the absorption time scale $\tau = \hbar/(2\varepsilon)$. The recoil thus involves an electron acceleration of $a = 2\varepsilon^2/(\hbar mc)$ over a time period of τ. The power of emission from an accelerating classical charge in the non-relativistic limit is given by the Larmor formula [JAC75]

$$P = \frac{2}{3}\frac{e^2}{4\pi\epsilon_0}\frac{a^2}{c^3} = \frac{2\alpha\hbar c a^2}{3c^3}. \quad \text{(IV.1)}$$

The electromagnetic energy emitted by the electron during the acceleration phase of the attempted absorption is therefore

$$E = \frac{2\alpha\hbar c a^2\tau}{3c^3} = \frac{2\alpha\hbar c}{3c^3}\frac{4\varepsilon^4}{(\hbar mc)^2}\frac{\hbar}{2\varepsilon} = \frac{4\alpha}{3}\frac{\varepsilon^3}{(mc^2)^2}. \quad \text{(IV.2)}$$

In the low-energy limit, conservation of energy can be re-established by the emission of a photon of energy ε during the acceleration phase. To estimate the probability of such an emission we assume: emission during the acceleration phase of the electron recoil manifests itself as a single photon of energy ε, and the probability of emitting such an energy and momentum conservation-reestablishing real photon from an individual recoiling electron is given by the total classical energy emission [see Eq. (IV.2)] divided by the energy of the required photon. The corresponding emission probability is given by

$$\mathrm{P} = \frac{4\alpha}{3}\frac{\varepsilon^2}{(mc^2)^2} = \frac{4\alpha}{3}\frac{v^2}{c^2}. \qquad \text{(IV. 3)}$$

The initial absorption attempt can only be successful if the energy and momentum conservation-reestablishing photon emission occurs. The corresponding absorption and emission (scattering) cross section is given by

$$\sigma = P\alpha\pi\lambda\!\!\!^{-2} = \frac{4\alpha}{3}\frac{\varepsilon^2}{(mc^2)^2}\frac{\alpha\pi(\hbar c)^2}{\varepsilon^2} = \frac{4\pi\alpha^2\lambda\!\!\!^{-2}_{\mathrm{C}}}{3}. \qquad \text{(IV. 4)}$$

The third step is to realize that Eq. (IV.4) is only half the Compton cross section, because in obtaining Eq. (IV.4), the photon absorption is assumed to occur before the recoil-induced photon emission. However, via the time-energy uncertainty principle, the order of these processes can be reversed; i.e. it is also possible for an isolated electron to spontaneously accelerate, emitting a photon of energy ε, in the presence of an incident real photon of energy ε, but before the absorption of the incident photon. This spontaneous acceleration and emission violates conservation of energy and momentum, but via quantum mechanics is allowed to occur for a time scale of $\tau = \hbar/(2\varepsilon)$ before the incident photon is absorbed, re-establishing conservation of energy and momentum. This is the same effect as in standard second-order QED where two Feynman diagrams are needed [BJO64, pg 128] (see Fig. IV.1) to calculate the Compton cross section. This effect doubles Eq. (IV.4), giving our final result for the Compton cross section

$$\sigma_{\mathrm{C}} = \frac{8\pi\alpha^2\lambda\!\!\!^{-2}_{\mathrm{C}}}{3}. \qquad \text{(IV. 5)}$$

The arguments presented here are not meant to supersede or replace standard QED, but perhaps can be used to give physicists with little or no background in QED, a simplified picture which captures some essence of the Compton scattering process. The presence of such a simple picture supports the suggestion that a doorway cross section of $\alpha\pi\lambda\!\!\!^{-2}$ plays a role in some QED processes.

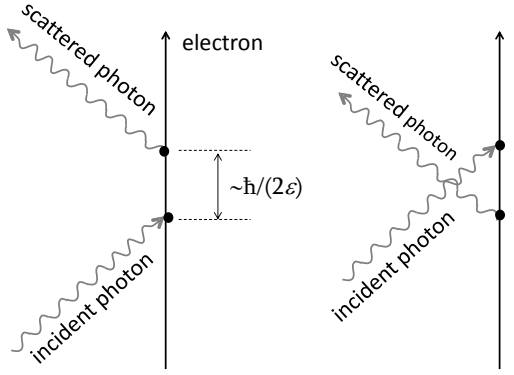

Fig. IV.1. The two second-order Compton scattering Feynman diagrams.

The simple Compton scattering mechanism introduced above is inconsistent with the constant and instantaneous recoil velocity assumed in section III to obtain the Lamb shift. We accept that simple semi-classical pictures of different processes may need to use different assumptions that capture the different essences of these processes. Our picture of the Lamb shift requires acknowledgement of a recoil velocity and the corresponding displacement, but not the corresponding acceleration associated with the velocity change. Our picture of Compton scattering needs us to acknowledge the electron's acceleration associated with photon absorption, but does not require us to consider any physical spatial displacement of the electron. Perhaps these are related to the Lamb shift being an energy shift associated

with electron displacements (but not accelerations), while the Compton cross section's size is related to the acceleration of the recoil (but not dependent on its displacement for free electrons). An interplay between our knowledge of displacement and acceleration may be due to a combined effect of both the position-momentum, and time-energy uncertainty principles. If an acceleration exists for a time τ then conservation of energy can be violated by $\sim \hbar/(2\tau)$. Dividing the position-momentum uncertainty principle by τ gives $\Delta x \cdot m \cdot \Delta a \sim \hbar/(2\tau)$, where Δa is the uncertainty of the acceleration operating over the time interval τ. For macroscopic time intervals with τ approaching infinity, both displacement and acceleration can be simultaneously known to high accuracy. However, for the recoils of mass m objects associated with the absorption of individual photons with energies $<< mc^2$, the equation $\Delta x \cdot m \cdot \Delta a \sim \hbar/(2\tau)$ implies that either the corresponding displacement or the acceleration can be known accurately, but not both simultaneously. Perhaps this is related to why, for the Lamb shift, we can assume a constant recoil velocity with no reference to an electron's acceleration, while for Compton scattering we can assume a constant acceleration with no reference to an electron's displacement.

V. Anomalous magnetic moment of the electron

To obtain a simple picture of the anomalous magnetic moment of a free electron, we are at first guided by the fact that in QED the anomalous magnetic moment is caused by the emission and reabsorption of virtual photons. We introduce: the stimulated emission, at the end of the Lamb shift related recoil, can be reabsorbed by the electron after its instantaneous jump back to its original location (see Fig. V.1).

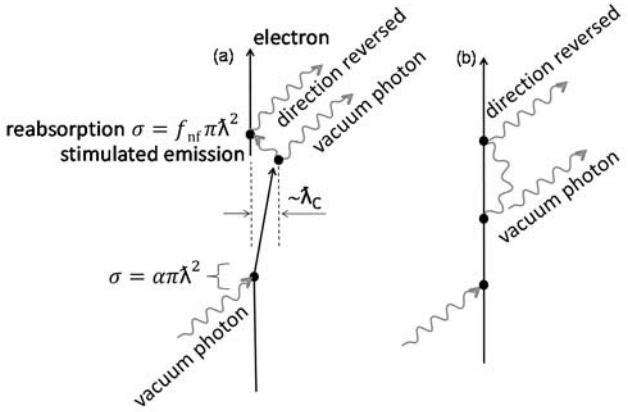

Fig. V.1. Feynman-like diagram for the reaction mechanism used here to obtain a simple representation of the anomalous magnetic moment of the free electron. (a) Almost the same diagram as shown in Fig. III.1. The only difference is that the stimulated virtual photon emitted at the end of the electron recoil "finds" the electron soon after its "return" to its pre-recoil location. After the reabsorption, the stimulated virtual photon is re-emitted in the reverse direction. This process is discussed in sections VI through VIII. Straightening out the electron's path gives the diagram to the right (b). Removing the ingoing and outgoing virtual photons gives the standard Feynman diagram for the anomalous magnetic moment.

We assume the cross section for the reabsorption of a stimulated virtual photon is $\pi\lambda\!\!\!^{-2}$ if the distance between the birth and reabsorption locations d is very much larger than $\lambda\!\!\!^{-}$, but with a new high-energy reabsorption cutoff, $\varepsilon_R < \varepsilon_H$, that is influenced by the state of the electron. The corresponding reabsorption probability is $P = \pi\lambda\!\!\!^{-2}/(4\pi d^2)$. We assume the high-energy reabsorption cutoff ε_R is inversely proportional to the wavelength of the electron, and therefore quasi-free electrons in a macroscopic trap have a very small high-energy reabsorption cutoff. Here we have used the term "reabsorption" to characterize the process where a photon "finds" an electron via its interaction cross

section. In section II.C the term "self-absorption" was used to characterize the semi-classical return of a stimulated virtual photon following the time scale set by the time-energy uncertainty principle. These two modes of absorbing a virtual photon are different. Later, we will introduce the idea that stimulated virtual photons are not terminated by absorption, but absorption is followed by a direction-reversed emission as depicted in Fig. V.1.

Given the exponential distribution of Lamb-shift related recoil distances, the probability that a stimulated virtual photon emitted at the end of the recoil is reabsorbed is given by

$$P_{\mathrm{sa}} = \frac{\int_0^{\infty}\int_0^{\varepsilon_{\mathrm{R}}} \frac{\pi\lambda\!\!\!^{-2}}{4\pi x^2}\exp\left(\frac{-x}{\lambda\!\!\!^{-}_{\mathrm{C}}}\right) dx\, d\varepsilon}{\int_0^{\infty}\int_0^{\varepsilon_{\mathrm{R}}}\exp(-x/\lambda\!\!\!^{-}_{\mathrm{C}}) dx\, d\varepsilon} = \frac{1}{\lambda\!\!\!^{-}_{\mathrm{C}}\varepsilon_{\mathrm{R}}}\int_0^{\infty}\int_0^{\varepsilon_{\mathrm{R}}} \frac{\hbar^2 \mathrm{c}^2}{4x^2\varepsilon^2}\exp\left(\frac{-x}{\lambda\!\!\!^{-}_{\mathrm{C}}}\right) dx\, d\varepsilon\,. \qquad (\mathrm{V}.1)$$

This is further simplified by switching to a length scale in units of $\lambda\!\!\!^{-}_{\mathrm{C}}$ and an energy scale of mc^2, giving

$$P_{\mathrm{sa}} = \int_0^{\infty}\int_0^{\varepsilon_{\mathrm{R}}} \frac{1}{4x^2\varepsilon^2}\exp(-x)\frac{dx\, d\varepsilon}{\varepsilon_{\mathrm{R}}}\,. \qquad (\mathrm{V}.2)$$

This gives the unphysical result of an infinite probability due to the $1/x^2$ term. This situation can be rectified by the realization that near-field effects will introduce an effective low-energy cutoff by modifying the absorption cross section for photons "falling" towards an electron from a finite starting distance d. The reabsorption cross section of $\pi\lambda\!\!\!^{-2}$ for $d >> \lambda\!\!\!^{-}$, is consistent with the effective semi-classical photon-electron interaction size of $\lambda\!\!\!^{-}$ (see Fig. II.1). Near-field effects should start growing rapidly as the separation decreases through ~$2\lambda\!\!\!^{-}$, and be strong for photons starting a distance $d < \lambda\!\!\!^{-}$, with the photons increasingly losing their ability to interact with the particle as d decreases towards zero. This gives the result that, as $d \to 0$, a photon has no time (and/or space) to be absorbed, and fails to interact with the nearby particle. In an attempt to include near-field effects we introduce: absorption proceeds via a distribution of effective absorption sites around each electron. We speculate this distribution of absorption sites is given by $\exp(-r^2/(2\lambda\!\!\!^{-2}))$ (the harmonic oscillator ground-state wave function). The absorption amplitude per unit distance traveled by the photon is assumed to be proportional to the density of absorption sites. The absorption cross section for a photon starting a distance d from an electron is then given by

$$\sigma_{\mathrm{nf}}(\lambda\!\!\!^{-}, d) = \left|\frac{2}{\lambda\!\!\!^{-}\sqrt{2\pi}}\int_0^{d}\exp\left(\frac{-r^2}{2\lambda\!\!\!^{-2}}\right)dr\right|^2 \pi\lambda\!\!\!^{-2} = \mathrm{erf}^2\left(\frac{d}{\lambda\!\!\!^{-}\sqrt{2}}\right)\pi\lambda\!\!\!^{-2} = f_{\mathrm{nf}}\,\pi\lambda\!\!\!^{-2}, \qquad (\mathrm{V}.3)$$

for photon energies < ε_{R}. Including Eq. (V.3) leads to the finite result

$$P_{sa} = \int_0^{\infty}\int_0^{\varepsilon_{\mathrm{R}}} \mathrm{erf}^2\left(\frac{x\varepsilon}{\sqrt{2}}\right)\exp(-x)\frac{dx\, d\varepsilon}{4x^2\varepsilon^2\varepsilon_{\mathrm{R}}}\,. \qquad (\mathrm{V}.4)$$

For a very low-energy electron (in a large macroscopic trap), we set the cutoff energy ε_{R} to zero and rewrite Eq. (V.4)

$$P_{sa} = \int_0^{\infty}\int_0^{\varepsilon_{\mathrm{R}}} \frac{4x^2\varepsilon^2}{2\pi}\exp(-x)\frac{dx\, d\varepsilon}{4x^2\varepsilon^2\varepsilon_{\mathrm{R}}} = \frac{1}{2\pi}\,. \qquad (\mathrm{V}.5)$$

This is reminiscent of the second-order QED value of $\alpha/(2\pi)$ for $(g-2)/2$. This result can be obtained with: reabsorption of a stimulated virtual photon enables the generation of a magnetic moment of one Bohr magneton, μ_{B}, in the direction of the electron's spin for a time period equal to the average spacing between reabsorption attempts $t = \pi\hbar/\varepsilon_{\mathrm{R}}$; and this magnetism is in addition to the standard intrinsic magnetic moment associated with the Dirac equation. We have no strong plausibility arguments for these assumptions other than invoking them gives the desired results presented below. The reabsorption process responsible for the anomalous magnetic moment of the free electron is depicted in Fig. V.1. As discussed previously, the rate of stimulated virtual photon emission following a recoil is $\alpha\varepsilon_{\mathrm{H}}/(\pi\hbar)$. Only

$\varepsilon_R/\varepsilon_H$ of this emission is available for reabsorption with only $1/(2\pi)$ of these reabsorption attempts being successful. Including the magnetic-moment generation time introduced above, the average anomalous magnetic moment of the free electron is

$$\bar{\mu}_e = \frac{\alpha\varepsilon_H}{\pi\hbar}\frac{\varepsilon_R}{\varepsilon_H}\frac{1}{2\pi}\cdot 1\mu_B \cdot \frac{\pi\hbar}{\varepsilon_R} = \frac{\alpha}{2\pi}\mu_B\,, \qquad (V.6)$$

in agreement with second-order QED. It may appear as if unjustified assumptions have been made to generate the correct answer. However, the proposed reaction mechanisms can be tested by the calculation of its additional consequences as done below. Before moving on to a calculation of the fine-structure constant, we attempt an "explanation" of the change in the magnetic moment associated with electrons in hydrogen-like atoms (ions) as a function of the charge of the atomic nucleus.

V.A Magnetic moment of the electron in hydrogen-like systems

The interplay between the far-field absorption cross section and near-field effects gives the result that, even in the limit as the size of the electron recoil goes to zero, $1/(2\pi)$ of the stimulated emissions with $\varepsilon \le \varepsilon_R$ are reabsorbed. This leads to the interesting possibility that $1/(2\pi)$ of the stimulated emissions following recoilless interactions (see Fig. II.2) with $\varepsilon \le \varepsilon_R$ are initially reabsorbed (and then re-emitted in the reverse direction as discussed later). If true, the total rate of reabsorptions would be $\varepsilon_R/(\pi\hbar)/(2\pi)$ with a fraction α following recoils associated with the Lamb shift, and $1-\alpha$ following recoilless interactions with vacuum photons. If those following the Lamb-shift-related recoils generate magnetism then so might all reabsorptions. However, all of the magnetic moment of the electron has been accounted for, with the intrinsic value from the Dirac equation plus the anomalous value from the previous section. We solve this problem by assuming any magnetic moment generated by the reabsorptions following recoilless vacuum-photon interactions is a part of the intrinsic magnetic moment associated with the Dirac equation. This assumption appears unorthodox, and gives a breakdown of the magnetic moment of the free electron as displayed in Fig. V.2. Notice that $\mu_B/(2\pi)$ of the magnetic moment is due to the emission and reabsorption of stimulated virtual photons. This component is divided into two parts. For free electrons, these are $\alpha\mu_B/(2\pi)$ and $(1-\alpha)\mu_B/(2\pi)$. The $\alpha\mu_B/(2\pi)$ component is associated with the emission and reabsorption following the displacement of the electron that causes the Lamb shift, and is the anomalous magnetic moment in excess of the intrinsic magnetic moment associated with the Dirac equation. The $(1-\alpha)\mu_B/(2\pi)$ component is also initiated by vacuum virtual photons, but associated with interactions with no consequence on the Lamb shift, and assumed to be a part of the intrinsic magnetic moment. The $\alpha\mu_B/(2\pi)$ component varies with the properties of the electron trap via the high-energy reabsorption cutoff, ε_R. This dependency on the state of the electron can be determined via Eq. (V.4). We assume that the $(1-\alpha)\mu_B/(2\pi)$ component has the same dependence on the properties of the electron trap.

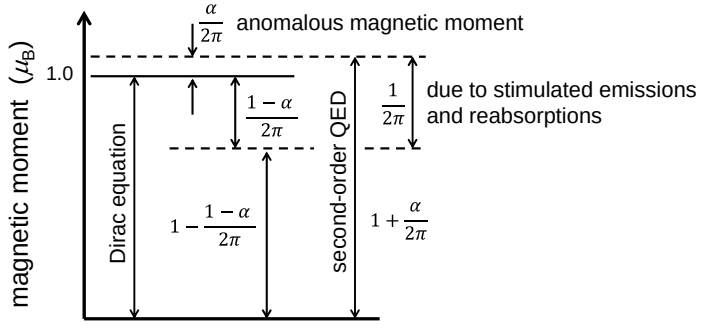

Fig. V.2. Different components of the magnetic moment of the free electron.

The reabsorption probability of exactly $1/(2\pi)$ in Eq. (V.5) is obtained via the assumption of a large macroscopic trap. Hydrogen-like atoms (ions) can be viewed as microscopic traps with a diameter (size) twice the corresponding Bohr radius. Based on the discussion in the previous subsection, the size of the high-energy reabsorption cutoff will increase with the electron's momentum, and thus increase with the atomic number of the nucleus of a hydrogen-like atom. This shift in the cutoff energy to higher values decreases the calculated magnetic moment of the electron because, at higher photon energies, the error function in Eq. (V.4) becomes increasingly lower than the corresponding low-energy limit used to obtain Eq. (V.5). A reasonable representation of the electron's magnetic moment as a function of the atomic number of the nucleus in a hydrogen-like atom can be obtained by adding the assumption: the high-energy cutoff for the stimulated-virtual-photon reabsorption cross section is given by the energy of a photon whose wavelength is twice the distance of the electron from the associated partner particle; i.e. $\varepsilon_R = hc/(2d) = \pi\hbar c/d$. For electron-nucleus ground-state systems, we replace d with the corresponding Bohr radius, giving $\varepsilon_R = \alpha\pi Zmc^2$. Incorporating this into Eq. (V.4) gives

$$P_{sa} = \int_{x=0}^{\infty}\int_{\varepsilon=0}^{\alpha\pi Z}\frac{4x^2\varepsilon^2}{2\pi}\left(1-\frac{x^2\varepsilon^2}{3}+\cdots\right)\exp(-x)\frac{dx\,d\varepsilon}{4x^2\varepsilon^2\alpha\pi Z} = \frac{1}{2\pi}-\frac{\pi}{3}\frac{\alpha^2Z^2}{3}. \qquad (V.7)$$

Including the other assumptions discussed above, Eq. (V.7) translates into a Z dependence of the geomagnetic ratio of hydrogen-like atoms of

$$g(1s)(\text{semiclassical}) = 1-\frac{1-\alpha}{2\pi}+\frac{1}{2\pi}-\frac{\pi}{3}\frac{\alpha^2Z^2}{3} \sim g_e\left[1-\frac{\pi}{3}\frac{\alpha^2Z^2}{3}\right]. \qquad (V.8)$$

The standard Dirac-equation based calculation of the corresponding quantity, to the same order, is [GRO70]

$$g(1s) = g_e\left[1-\frac{\alpha^2Z^2}{3}\right]. \qquad (V.9)$$

Eq. (V.9) predicts that the magnetic moment of an electron in a hydrogen atom differs from that of a free electron by −17750 ppb (parts per billion). The corresponding experimental value is −17709(13) ppb [TIE77]. The small disagreement between Eq. (V.9) and experiment is due to higher-order and nuclear-mass correction terms [GRO70] not included here. The simple method presented here gives a $g(1s)$ α^2Z^2 coefficient that is 4.6% higher than the correct result [see Eq. (V.9)]. This comparison to the expectation from standard theoretical considerations partially justifies the above assumptions, while highlighting a real difference for which we have no explanation at the present time.

VI. Exchange of virtual photons between an electron pair

A stimulated-virtual-photon reabsorption probability by an isolated electron is used in section V to obtain the anomalous magnetic moment of the electron. In the case of an electron pair, the same reabsorption process should enable the stimulated emission from one electron to be absorbed by the partner, thus enabling an exchange of photons between an electron pair. In such an exchange, both the emission and absorption of the stimulated virtual photon would be completely suppressed by energy conservation if only classical physics was assumed. We temporarily ignore this important fact and use the emission rate given by Eq. (II.2) and a stimulated-virtual-photon absorption cross section of $\pi\lambda\!\!\!^{-2}$ (for $\varepsilon < \varepsilon_R = \pi\hbar c/d$, as from section V) to calculate the repulsive force associated with the exchange of stimulated virtual photons between an electron pair

$$F = 2\int_0^{\varepsilon_R}\frac{d\varepsilon}{\pi\hbar}\frac{\varepsilon}{c}\frac{\pi\lambda\!\!\!^{-2}}{4\pi d^2} = \frac{\hbar c}{2\pi d^2}\int_0^{\varepsilon_R}\frac{d\varepsilon}{\varepsilon}. \qquad (VI.1)$$

The factor of two is because of the two-way exchange of the photons between the pair. We have assumed the exchange of the stimulated virtual photon generates a momentum change of ε/c in the emitting/absorbing particle, away from the absorbing/emitting partner. The integral in Eq. (VI.1) is reminiscent of that used to obtain the Lamb shift is section III. A depiction of the virtual-photon exchange between a pair of electrons is presented in Fig. VI.1.

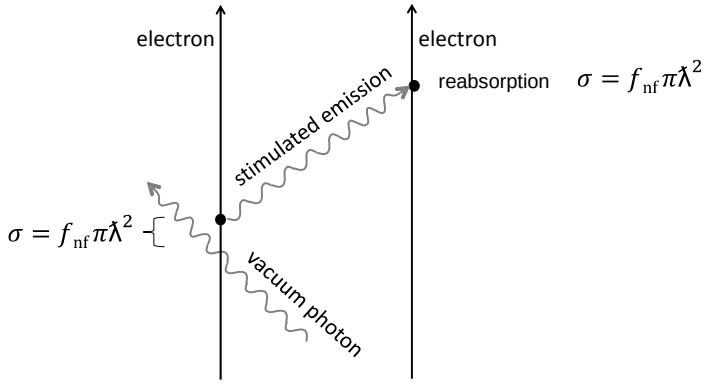

Fig. VI.1. Feynman-like diagram depicting the exchange of a virtual photon between an electron pair. This is almost the same as Fig. II.2 except here the stimulated virtual photon terminates on a partner electron.

The lack of a low-energy cutoff in Eq. (VI.1) leads to an infinite force. To obtain a finite force, we need only include the low-energy cutoff associated with near-field effects, introduced in the previous section. If an attempted exchange were to be initiated, the absorption cross section would be reduced via the near-field effect discussed in section V, and given by Eq. (V.3). Perhaps less obvious, the cross section used to calculate the emission rate for initiating the exchange must also be multiplied by the error-function squared term from Eq. (V.3). This can be justified by time-symmetry arguments that apply equally to emission and absorption processes; i.e. in the case of a photon exchange between two electrons, the cross section for the stimulated emission (the emission rate) is influenced by the presence of the partner electron by the same factor that modifies the absorption cross section due to the presence of the partner. This is required because incident photons with $\lambda\!\!\!^{-} >> d$ cannot recognize the individual electrons in the pair, but instead see them as a collective object, and thus cannot generate stimulated photons that cause the recoil of an individual electron, but instead cause the pair to recoil as a whole. The near-field effects considered here are analogous to the interaction properties of closely spaced classical antennas [IRA08].

The absorption by the partner electron re-establishes conservation of energy and momentum but only after an exchange time of $t_{\rm ex} = d/c$. As discussed in section II the probability that a stimulated virtual photon, is still "heading outwards" in search of a partner after a time t is given by $\exp(-t/\tau)$ with $\tau = \hbar/(2\varepsilon)$. Substituting in the exchange time gives a photon-exchange flux-reduction factor of $f = \exp(-\varepsilon/T_{\rm ex})$ with an effective exchange temperature of $T_{\rm ex} = \hbar c/(2d)$. Assuming this factor applies, and including the near-field effects discussed above, the flux of virtual photons emitted from one electron, available for absorption by a partner (different) electron, per unit solid angle, is given by [see Eq. (II.2)]

$$f_{\rm ex}(\lambda\!\!\!^{-}, d) = \frac{1}{4\pi}\int_0^{\varepsilon_{\rm R}} \mathrm{erf}^2\left(\frac{d}{\lambda\!\!\!^{-}\sqrt{2}}\right)\exp(-\varepsilon/T_{\rm ex})\frac{d\varepsilon}{\pi\hbar}. \qquad \text{(VI. 2)}$$

The corresponding force between two electrons is

$$F = 2\frac{1}{4\pi}\int_0^{\varepsilon_{\rm R}=\pi\hbar c/d} \mathrm{erf}^2\left(\frac{d}{\lambda\!\!\!^{-}\sqrt{2}}\right)\exp(-\varepsilon/T_{\rm ex})\frac{d\varepsilon}{\pi\hbar}\frac{\varepsilon}{c}\mathrm{erf}^2\left(\frac{d}{\lambda\!\!\!^{-}\sqrt{2}}\right)\frac{\pi\lambda\!\!\!^{-2}}{d^2}. \qquad \text{(VI. 3)}$$

Switching into energy in units of $T_{\rm ex} = \hbar c/(2d)$ gives the more compact result

$$F = \frac{\hbar c}{2\pi d^2}\int_0^{2\pi}\frac{\mathrm{erf}^4\left(\varepsilon/2^{3/2}\right)}{\varepsilon}\exp(-\varepsilon)\,d\varepsilon, \qquad \text{(VI. 4)}$$

and thus an estimate of the fine-structure constant of

$$\alpha = \frac{1}{2\pi}\int_0^{2\pi}\frac{\mathrm{erf}^4\left(\varepsilon/2^{3/2}\right)}{\varepsilon}\exp(-\varepsilon)\,d\varepsilon = \frac{1}{168.865\ldots}, \qquad \text{(VI. 5)}$$

with a corresponding fundamental unit of charge of 1.44×10^{-19} C.

If the suggestions used here are on the right track, then the significant difference between Eq. (VI.5) and experiment indicates the need for an additional process that can enhance the photon exchange. Such an enhancement can be obtained by assuming absorption by the partner particle generates a direction-reversed stimulated emission. This is reminiscent of the stimulated emission of photons with a probability of $\exp(-\varepsilon/T)$ following the absorption of an incident photon on a black hole [BEK77]. For a small black hole with a very high temperature, the stimulated emission probability of low-energy photons is unity. In the exchange of virtual photons between an electron pair, we assume the absorption of the first exchange generates a direction-reversed virtual photon that, in the case of a weakly-interacting pair, is emitted in a direction to find the partner particle with a jump probability controlled by only the time-energy uncertainty principle; i.e. with a probability of making the jump back across the distance d, given by $f = \exp(-\varepsilon/T_{ex})$ (just as in the original exchange). This second exchange, in turn, generates an additional exchange with a further reduction of f, and so forth. The combined effect of these multiple direction-reversing exchanges gives a factor of $f + f^2 + f^3 + \ldots = f/(1-f) = 1/[\exp(\varepsilon/T_{ex})-1]$ instead of the $\exp(-\varepsilon/T_{ex})$ term in Eq. (VI.5). Assuming this factor, Eq. (VI.5) becomes

$$\alpha = \frac{1}{2\pi}\int_0^{2\pi}\frac{\mathrm{erf}^4\left(\varepsilon/2^{3/2}\right)}{\varepsilon[\exp(\varepsilon)-1]}d\varepsilon = \frac{1}{139.713\ldots}, \qquad \text{(VI. 6)}$$

with a corresponding fundamental unit of charge of 1.587×10^{-19} C. This is incorrect by ~1%. A difference of this size might be due to higher-order corrections not considered is this section.

It may appear as though there is an inconsistency between the use of the erf^4 term in Eq.s (VI.4) through (VI.6) and the erf^2 term in Eq. (V.4). In the calculation of the anomalous magnetic moment of the electron we use the erf^2 term to modify the reabsorption cross section, because the relevant photons have knowledge of both the birth and reabsorption locations, and thus the separation distance d. In the case of the anomalous magnetic moment, the initial stimulated emission is on a single isolated electron and we thus assume the unmodified cross section of $\pi\lambda\!\!\!^{-2}$. In the case of a photon exchange, both the emission and absorption events are aware of the location of the corresponding partner electron.

The force associated with the semi-classical exchange of virtual photons between two particles introduced here can only generate repulsion. However, an attractive force between oppositely charged particles can be obtained by assuming the opposite charge is associated with a hole in a Fermi-sea of negative-energy particles [BJO64, chap. 5].

VI.A Transition from quantum to classical behavior

The nature of the semi-classical virtual-photon exchange discussed above can be approximately characterized by a photon of energy $\varepsilon \sim \hbar c/d$ being exchanged every $\tau \sim d/(\alpha c)$; i.e. a photon with a reduced wavelength near the separation distance between the particles, with the time period between exchange events near the photon transit time multiplied by $1/\alpha$. Each exchanging photon exists for the transit time $t=d/c$, with the probability that an exchange is in progress at any instant being $\sim\alpha$. Classical-like behavior will be obtained if the displacement caused by a single exchange is much smaller than the separation distance of the particle pair; and if the particle-energy change from a single exchange is much

smaller than the system's potential energy. To estimate an approximate system size for the boundary between quantum and classical behavior we consider a stationary electron at a distance d from a massive particle of the same charge. On the emission or absorption of an exchanged photon, the electron's velocity changes to $v=\varepsilon/(mc)\sim\hbar/(md)$. The corresponding displacement between exchanges is $\Delta d \sim \hbar/(md)\times d/(\alpha c) = \lambda\!\!\!^{-}_C/\alpha$ (the Bohr radius). For the electron to effectively sense the electric potential as a classical-like object (i.e. continuously along its path) we need $\Delta d << d$, and thus classical-like behavior occurs at particle separation distances very much larger than the size of atoms. Similarly, the kinetic energy of an initially stationary electron after a single absorption or emission of an exchanged photon is $E_k = mv^2/2 \sim \hbar c\lambda\!\!\!^{-}_C/(2d^2)$. This must be very much less than the potential energy $V=\alpha\hbar c/d$, if we desire classical-like behavior, where the electron accelerates smoothly to its final energy. The corresponding condition for classical-like behavior is $d >> \lambda\!\!\!^{-}_C/(2\alpha)$. Again, we get the result that the interaction is classical-like for interaction distances much larger than the size of atoms. Notice that the Bohr radius shows up as the transitional length scale between classical and quantum behavior without the use of the electron's de Broglie wave length.

It is possible that if the semi-classical calculations performed here are replaced with more detailed calculations then several of the semi-classical features may disappear, with only the fine-structure constant surviving with a smooth classical-like potential. This would negate the arguments presented in this section, and perhaps be more conducive of the smooth electron path assumed in the next section to obtain the Larmor formula.

VII. Larmor formula

In the above section, we suggested a mechanism where charge might be an emergent property associated with the exchange of virtual photons between a pair of point particles. A value near the universal charge of $\sim 1.6\times10^{-19}$ C is obtained by imagining a direction-reversing stimulated-emission process that causes virtual photons to "rattle" between a particle pair. In this speculative model a particle can initiate a photon exchange which "jumps" across the separation distance d in a time of d/c. Previously, a weak interaction between an electron pair (at large separation distances) was invoked, where the acceleration of the particles could be ignored with the direction-reversed emission assumed to "automatically" find the partner particle with a jump probability controlled by only the time-energy uncertainty principle. This would require the particle pair and the exchanging photon to be in some sort of entangled state where the direction-reversing stimulated-emission process "knows" which direction to send the emitted photon so it finds the partner particle. However, if the particle is accelerating there might be a mismatch in the returning photon's size and the accelerating particle's location relative to those associated with the "automatic" absorption in the case of non-accelerating particles. This might, in turn, lead to some of the returning virtual photon's energy being scattered (or absorbed and re-emitted) to infinity as real emission. This mechanism is used here to obtain a result close to the Larmor formula for the power of electromagnetic emission from an accelerating electron.

To study the effect of an acceleration a of a point particle of mass m, we place a massive point charge a distance $d_0=[\alpha\hbar c/(ma)]^{1/2}$ with the same velocity as the accelerating particle at $t_0=0$. Fig. VII.1 is a Feynman-like diagram that depicts a double exchange. We assume the accelerating charge initiates an exchange with the massive particle at $t_0=0$. This exchange takes a time $t_1=d_0/c$. If there was no acceleration (and no initial velocity), the return time of a direction-reversed stimulated emission, t_2-t_1, back to the particle of mass m, would be the same. However, the acceleration increases this time to

$$t_2 - t_1 = \frac{d_0}{c}(1 + 2\beta + 4\beta^2), \tag{VII.1}$$

to second order, where $\beta = ad_0/c^2$. The corresponding square of d_0 relative to the return distance d is

$$\left(\frac{d_0}{d}\right)^2 = 1 - 4\beta + 4\beta^2. \tag{VII.2}$$

This factor is the relative change in the angular size of the electron as viewed from the origination site of the direction-reversed emission, relative to the case of a non-accelerating electron.

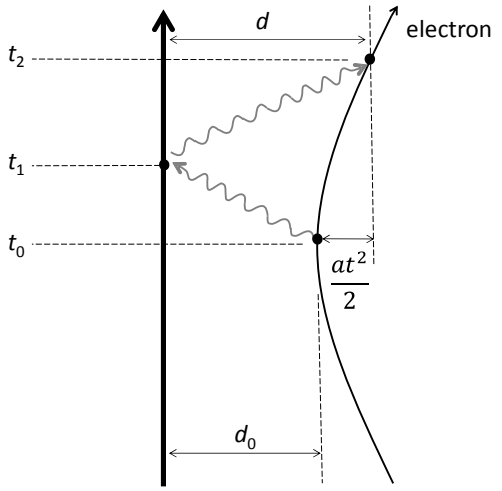

Fig. VII.1. A depiction of double photon exchange near the electron's turning point. The bold line represents the "stationary" massive particle moving through time.

At the time of absorption at the end of the double exchange depicted in Fig. VII.1, the accelerating particle is moving with a speed of $v/c = 2\beta + 2\beta^2$. Due to the corresponding Doppler shift, the effective reduced wavelength of the absorbed photon relative to its original value is

$$\left(\frac{\lambda\!\!\!^{-}}{\lambda\!\!\!^{-}_0}\right)^2 = 1 + 4\beta + 4\beta^2. \tag{VII.3}$$

to second order (including relativistic effects). This factor is the relative change in the size of direction-reversed photons as viewed by the electron, relative to the case of a non-accelerating electron. Combining Eq.s (VII.2) and (VII.3) gives a relative change in the photon-electron effective interaction size, relative to the case of a non-accelerating electron of

$$\left(\frac{d_0\lambda\!\!\!^{-}}{d\lambda\!\!\!^{-}_0}\right)^2 = 1 - 8\beta^2. \tag{VII.4}$$

We assume that this effective size change, due to acceleration, causes $8\beta^2$ of the direction-reversed photon energy to be scattered towards infinity as a potential real photon. Eq. VII.4 is obtainable (in the non-relativistic limit) with initial exchanges not at the electron's turning point as depicted in Fig. VII.1.

The force from Eq. (VI.4) is modified by the direction-reversing stimulated emission to

$$F = \frac{\hbar c}{2\pi d^2}\int_0^{2\pi} \frac{\mathrm{erf}^4\left(\varepsilon/2^{3/2}\right)[1-\exp(-\varepsilon)+\exp(-\varepsilon)]}{\varepsilon\,[\exp(\varepsilon)-1]}\,d\varepsilon = \frac{\alpha\hbar c}{d^2}. \tag{VII.5}$$

The positive and negative $\exp(-\varepsilon)$ in Eq. (VII.5) looks redundant. However, the $1-\exp(-\varepsilon)$ term is associated with the first (initial) exchanges, while the $\exp(-\varepsilon)$ term is associated with the direction-reversed exchanges that might be influenced by the acceleration of the particles. The corresponding

electromagnetic power being exchanged from the massive charge to the accelerating electron (depicted in Fig. VII.1) can be expressed as

$$P = \frac{\hbar c^2}{4\pi d^2}\int_0^{2\pi}\frac{\mathrm{erf}^4(\varepsilon/2^{3/2})[1-\exp(-\varepsilon)+\exp(-\varepsilon)]}{\varepsilon\,[\exp(\varepsilon)-1]}\,d\varepsilon, \qquad \text{(VII.6)}$$

Given the assumptions associated with Eq. (VII.4), the corresponding power associated with the conversion of the direction-reversed virtual-photon energy into real photons is given by

$$P = \frac{\hbar c^2}{d^2}\frac{8\beta^2}{4\pi}\int_0^{2\pi}\frac{\mathrm{erf}^4(\varepsilon/2^{3/2})\exp(-\varepsilon)}{\varepsilon\,[\exp(\varepsilon)-1]}\,d\varepsilon$$
$$= \frac{2}{\pi}\int_0^{2\pi}\frac{\mathrm{erf}^4(\varepsilon/2^{3/2})\exp(-\varepsilon)}{\varepsilon\,[\exp(\varepsilon)-1]}\,d\varepsilon\; a^2\frac{\hbar}{c^2} = 1.0160\ldots\frac{2}{3}\alpha a^2\frac{\hbar}{c^2}. \qquad \text{(VII.7)}$$

This result is 1.6% higher than the Larmor formula, and is perhaps close enough that higher order effects might be capable of reducing the pre-factor on the RHS of Eq. (VII.7) to a value much closer to unity. Instead of using the experimentally known α on the RHS of Eq. (VII.7) with the pre-factor of 1.0160…, we can set the pre-factor to unity and use the LHS of Eq. (VII.7) to predict α using

$$\alpha = \frac{3}{\pi}\int_0^{2\pi}\frac{\mathrm{erf}^4(\varepsilon/2^{3/2})\exp(-\varepsilon)}{\varepsilon\,[\exp(\varepsilon)-1]}\,d\varepsilon\,. \qquad \text{(VII.8)}$$

The corresponding predicted value of the universal charge is 1.615×10^{-19} C. This is close to the value of 1.587×10^{-19} C obtainable from Eq.s (VII.5) and (VI.6). These results suggest the inclusion of higher-order effects will increase the force between charges while decreasing the radiative power associated with acceleration. We notice that the pre-factor of 1.0160… in Eq. (VII.7) can be reduced to very close to unity by assuming $1-\alpha/(2\pi)$ of the Larmor emissions are reabsorbed by the electron, with an additional $1-2\alpha$ reabsorbed by the particle pair (as a collective object).

VII.A Radiation resistance (at low electron velocity)

An area of difficulty in electrodynamics has been to conserve energy in the presence of Larmor emissions. The problem occurs because the force that generates the initial electron acceleration conserves energy locally; i.e. the work done by the applied force goes into changing the state of the electron. However, the associated Larmor emissions to infinity then violate conservation of energy, unless a radiation resistance force is applied to the accelerating electron. This can be done by invoking the second term in the electron's self-reaction force as first determined by Lorentz [FEY62]. In the model presented here, the charge of an electron is an emergent property associated with the whole electron, and there is no mechanism for subdividing the electron into sub units which can interact with each other. The Larmor emission mechanism suggested here does not need a radiation resistance. Instead, the scattering of some of the exchanging photon energy to infinity automatically reduces the acceleration associated with the exchanging photons to conserve energy.

The energy spectrum of the direction-reversed exchanging photons is given by

$$P_{\mathrm{d}}(\varepsilon) \propto \frac{\mathrm{erf}^4(\varepsilon/2^{3/2})\exp(-\varepsilon)}{\varepsilon^2\,[\exp(\varepsilon)-1]}\,, \qquad \text{(VII.9)}$$

with energy in units of $T_{\mathrm{ex}}=\hbar c/(2d)$, and a mean energy of $\bar{\varepsilon}_{\mathrm{d}}=0.494\cdot\hbar c/d$. We suspect that higher-order corrections are likely to modify this result to be exactly $\bar{\varepsilon}_{\mathrm{d}}=\hbar c/(2d)$. As per Eq. (VII.4), $8\beta^2$ of the energy in a direction-reversed exchanging photon is scattered (preferentially about 90° to the particle pair's symmetry axis). In the case of a slow electron, the kinetic energy of the electron following the absorption of a single direction-reversed photon is (because of the favorable results that follow)

$$E_{\rm k} = \frac{\varepsilon_d^2}{2mc^2} - \varepsilon_{\rm d} 4\beta^2 = \varepsilon_d^2\left(\frac{1}{2mc^2} - \frac{4\beta^2}{\varepsilon_{\rm d}}\right). \qquad \text{(VII.10)}$$

The corresponding average momentum change associated with the absorption of a single direction-reversed photon is (to 2nd order)

$$\Delta\overline{p}_e \sim \frac{\overline{\varepsilon}_{\rm d}}{c}\left(1 - mc^2\frac{4\beta^2}{\overline{\varepsilon}_{\rm d}}\right) \sim \frac{\overline{\varepsilon}_{\rm d}}{c}\left(1 - mc^2\frac{8\beta^2 d}{\hbar c}\right) = \frac{\overline{\varepsilon}_{\rm d}}{c}\left(1 - 8\alpha^2\frac{\lambda\!\!\!^{-}_{\rm C}}{d}\right). \qquad \text{(VII.11)}$$

Notice that the correction due to acceleration is small even for separation length scales as small as $\sim\lambda\!\!\!^{-}_{\rm C}$. Also remember that, as per Lamb-shift physics, electrons cannot interact electromagnetically as effective point objects below this length scale. Similarly, the energy of a single Larmor photon cannot be larger than the potential energy of the particle pair. This means that, even though the Larmor emission power is obtained here by assuming it scatters off a localized semi-classical site (the electron), its wavelength is large enough that the emission must, in fact, come collectively from the particle pair.

The fraction of the repulsive force between two point-like particles mediated by the direction-reversed photons is given by

$$\left(\int_0^{2\pi}\frac{\text{erf}^4(\varepsilon/2^{3/2})\exp(-\varepsilon)}{\varepsilon\,[\exp(\varepsilon)-1]}\,d\varepsilon\right) / \left(\int_0^{2\pi}\frac{\text{erf}^4(\varepsilon/2^{3/2})}{\varepsilon\,[\exp(\varepsilon)-1]}\,d\varepsilon\right) = 0.1726\ldots, \qquad \text{(VII.12)}$$

and thus the reduction in the repulsion associated with the Larmor emission is given by

$$\overline{F}_{\rm r} \sim \frac{\alpha\hbar c}{d^2}0.1726\ldots\frac{8\alpha^2\lambda\!\!\!^{-}_{\rm C}}{d} = 1.381\ldots\frac{\alpha^3\hbar c\lambda\!\!\!^{-}_{\rm C}}{d^3}. \qquad \text{(VII.13)}$$

This is not the Lorentz force. We must remember, as pointed out by Feynman [FEY62], that the Lorentz formula is only valid for periodic motion, and the case we are considering here is far from periodic. Given the average time spacing between first exchanges is $\sim d/(\alpha c)$, the effective velocity by which (VII.13) needs to be multiplied to give the reduced work per unit time done to the electron (associated with the Larmor emission) is $v_{\rm r}\sim ad/(\alpha c)/2 = c\lambda\!\!\!^{-}_{\rm C}/(2d)$. Remember that here we are assuming the initial electron velocity (before the photon absorption) is zero. The corresponding reduction in the work per unit time done on the electron is

$$\overline{W}_{\rm r} \sim 1.381\ldots\frac{\alpha^3\hbar c\lambda\!\!\!^{-}_{\rm C}}{d^3}\frac{c\lambda\!\!\!^{-}_{\rm C}}{2d} = 0.6905\ldots\,\alpha a^2\frac{\hbar}{c^2}. \qquad \text{(VII.14)}$$

This is 1.95% higher than the Larmor emission power given by Eq. (VII.7). This discrepancy is removed by replacing the real α in Eq. (VII.14) by our estimate in Eq. (VI.6).

VII.B Radiation resistance (at higher electron velocity)

We now consider the case of an initial electron with a high radial velocity relative to the partner particle (but still non-relativistic) much larger than the velocity change associated with the absorption of the single exchanging photon. The results corresponding to Eq.s (VII.10) and (VII.11) are

$$E_{\rm k} = E_0 + \frac{\varepsilon_d^2}{2mc^2} - \varepsilon_{\rm d} 4\beta^2 + \varepsilon_{\rm d}\frac{v}{c}, \text{ and} \qquad \text{(VII.15)}$$

$$\Delta\overline{p}_e \sim \frac{\overline{\varepsilon}_{\rm d}}{c}\left(1 - 4\beta^2\frac{c}{v}\right), \qquad \text{(VII.16)}$$

where $E_0 = mv^2/2$ is the initial kinetic energy of the electron. The corresponding reduction in the repulsive force on the electron associated with the Larmor emission is given by

$$\overline{F}_{\mathrm{r}} \sim \frac{\alpha\hbar c}{d^2} 0.1726... \, 4\beta^2 \frac{c}{v} = 0.6905... \, \alpha a^2 \frac{\hbar}{c^2} \frac{1}{v}. \qquad \text{(VII.17)}$$

The corresponding reduction in the work per unit time done on the electron is obtained by multiplying by its velocity. This gives the same result as expressed in Eq. (VII.14).

VIII. Possible recoil corrections

In quantum field theory, if one tries to obtain a simple result, there is often a series of higher-order corrections. However, if not following a traditional path, it can be difficult to assess the type of higher-order effect that should be included next. We suggest that our calculated α given by Eq. VI.6 is lower that the experimental value because higher-order effects enhance the vacuum-photon induced stimulated-virtual-photon emission process depicted in figures II.2 and VI.1. We choose to be guided by the discrepancy between our calculated values of $(g–2)/2 = \alpha/(2\pi)$ and $\alpha^{-1} = 139.713$, and the corresponding experimental results. This is fraught with danger, given the simplistic methods used here to estimate the electron's anomalous magnetic moment and the fine-structure constant. For example, the discrepancy in the fine-structure-constant calculation might reflect the use of the sharp high-energy absorption cutoff, and might have little to do with the recoil corrections proposed below. Ignoring the possibility of adding confusion, we proceed with our analysis.

Assuming that a relatively simple correction factor can transform our calculated value of $\alpha^{-1} = 139.713$ into a value very close to the known experimental value, we write $\alpha^{-1} = 137.0359991 = 139.713/(1+a\alpha)^2$. The corresponding solution is $a = 1.332$. This is within 1-part per 1000 from 4/3, which is reminiscent of the 4/3 factor in the recoil correction needed to obtain the Compton cross section in section IV. Similarly, we write $(g–2)/2 = 0.001159652 = \alpha/(2\pi) \times (1–ab\alpha)$. Assuming $a = 4/3$, the corresponding solution is $b = 0.156$, within ~2% of $1/(2\pi)$, and reminiscent of the stimulated-virtual-photon reabsorption probability used to estimate the anomalous magnetic moment of the free electron in section V. These results may be fortuitous. However, we proceed to explore the possibility of electron-recoil based corrections to our calculated estimates of α and $(g–2)/2$. Before doing this it is beneficial to revisit the explanation of the electron's rest energy given in section II.

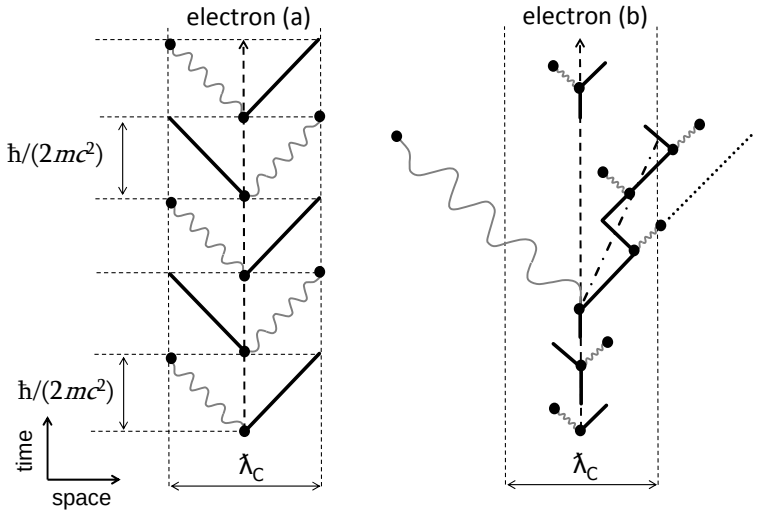

Fig. VIII.1. An extension of Fig. II.2, showing the repeated stimulated virtual-photon emissions responsible for the electron's rest energy. The stimulating vacuum virtual photons are not shown. (a) A simple representation where the stimulating vacuum virtual-photon energy is always mc^2 with the corresponding stimulations equally spaced in time. (b) An attempt to represent one of the complications associated with the spread in the stimulating vacuum photon energies (see text).

As per section II, the rest energy of a point particle is stored in the virtual-photon emissions stimulated by the passage of nearby vacuum virtual photons in the energy range from zero to $2\pi mc^2$. Each stimulated emission typically stores an energy of mc^2, these emissions are spaced in time by ~$\hbar/(2mc^2)$, and each lasts for a time period of ~$\hbar/(2mc^2)$. This is reminiscent of the Zitterbewegung obtained from the Dirac equation [BJO64, pg 38]. In the time period of ~$\hbar/(2mc^2)$ the stimulated virtual photon and the massless naked electron both recoil a distance $\hbar c/(2mc^2) = \lambda\!\!\!^{-}_C/2$, giving an effective electron size of ~$\lambda\!\!\!^{-}_C$ as depicted in Fig. VIII.1 part (a) (and as discussed in section II). In section III we learned that each recoil associated with the absorption of a real photon has a probability $P=4\alpha/3\times(v/c)^2$ of emitting a real photon of the same energy, where v is the recoil velocity. The recoils in Fig. VIII.1 part (a) associated with stimulated emissions have the same properties as recoils associated with the absorption of virtual photons. We thus suspect that each recoil in Fig. VIII.1 part (a) has a probability $P=4\alpha/3$ of emitting an additional virtual photon of the same energy. Notice that the recoil velocity of the massless "naked" electron in virtual absorptions is assumed to be c. This enhances the virtual-photon emission by a factor of $1+4\alpha/3$.

Fig. VIII.1 part (a) is an overly-simplistic view because the stimulated emissions are not uniformly spaced in time, and most $[1-1/(2\pi)]$ of the stimulated emissions will temporarily store more than mc^2, which lives for a time scale less than $\hbar/(2mc^2)$. A better, but still crude, depiction of the electron is given in Fig. VIII.1 part (b). In this figure, there are six high-energy stimulated emissions ($\varepsilon > mc^2$) for the one low-energy stimulated emission ($\varepsilon < mc^2$). As per the discussion about Fig. VIII.1 part (a), each of the recoils associated with the high-energy stimulated virtual emissions in Fig. VIII.1 part (b) must also have a probability of $P=4\alpha/3$ for generating an additional virtual emission. The rarer low-energy stimulated virtual emissions exist for a time scale much larger than the mean spacing between emission events, and extend about one-half of their reduced wavelength out from the center of the electron "cloud." This makes the exchange of low-energy stimulated virtual photons between an electron pair possible, as needed for the fine-structure-constant calculation presented in the previous section. The dotted line in Fig. VIII.1 part (b) shows the naked-electron's trajectory if the low-energy emission was not followed by several high-energy stimulated emissions. If this dotted recoil could exist, it would have a probability $P=4\alpha/3$ for generating an additional low-energy virtual emission. A more typical trajectory of the recoil following the low-energy emission is shown by the dash-dotted line. The multiple high-energy emissions following the low-energy emission cause this recoil to have an effective mass, and restrict the recoil of the naked-electron to a distance of ~$\lambda\!\!\!^{-}_C/2$, while the corresponding photon can travel ~$\lambda\!\!\!^{-}/2$. Despite the additional interactions in the recoiling electron, we still assume each low-energy stimulated emission has a probability $P=4\alpha/3$ of being associated with an additional virtual emission of the same energy. This additional virtual-photon emission process increases the stimulated virtual-photon emission by a factor of $1+4\alpha/3$ as depicted in Fig. VIII.2. As per the discussion in the previous subsection, time-symmetry arguments connect emission and absorption processes, and the emission enhancement must be mirrored by a corresponding enhancement on the absorption side of the photon exchange between an electron pair. These effects modify Eq. (VI.6) to

$$\alpha = \frac{(1+4\alpha/3)^2}{2\pi}\int_0^{2\pi}\frac{\mathrm{erf}^4\left(\varepsilon/2^{3/2}\right)}{\varepsilon[\exp(\varepsilon)-1]}d\varepsilon = \frac{(1+4\alpha/3)^2}{139.7129683\ldots}. \qquad \text{(VIII. 1)}$$

The corresponding solution is $\alpha^{-1}=137.0334$ with a calculated universal charge of 1.60219×10^{-19} C.

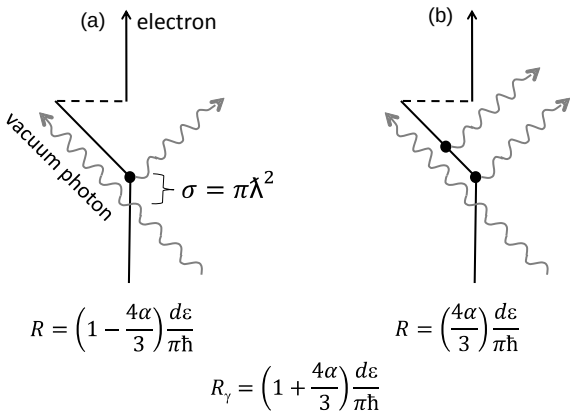

Fig. VIII.2. Two diagrams depicting recoil effects in vacuum-photon induced stimulated emission. The recoil generated by the first stimulated virtual photon is assumed to have a probability P=4α/3 for generating an additional virtual photon. Events as depicted in the left-hand diagram (a) occur at a rate given by Eq. (II.2) scaled by 1–4α/3 because the recoil in these events does not generate an additional virtual photon. The event rate for the right-hand diagram (b) is scaled by 4α/3 because of the presence of a recoil-induced additional virtual photon. These rates sum to Eq. (II.2), but the rate of vacuum-photon induced virtual emission is increased by a factor of 1+4α/3 relative to Eq. (II.2) because (b) contains two induced virtual-photon emissions.

Agreement with both the experimental α and (g–2)/2 values can be obtained by further invoking: events that contribute to the anomalous magnetic moment of the electron do not emit virtual photons. This can be seen by separating the relevant Feynman-like diagrams into those with and without the reabsorption of the stimulated virtual photons, as displayed in Fig. VIII.3. Parts (a) and (b) show events that occur with rates of 1−α and α [1−1/(2π)] times Eq. (II.2), respectively. The sum of these two rates is 1−α /(2π) times Eq. (II.2). Neither of these event classes contributes to the anomalous magnetic moment, and the recoil-induced emission is allowed with its full probability of 4α/3. Part (c) is an event type with a rate of α/(2π)×4α/3×1/(2π) times Eq. (II.2). In these events, the stimulated emission is reabsorbed with a probability of 1/(2π), and the corresponding recoil-induced emission is initially reabsorbed with a probability of 1/(2π) and then re-emitted direction reversed, via the mechanisms introduced in sections V.A and VI. The two reabsorptions in (c) generate the same magnetism, and we assume these are in opposite directions and cancel each other out. Therefore, event class (c) does not contribute to the anomalous magnetic moment, and the two direction-reversed emissions are allowed as displayed in (c). Part (d) shows events with a rate of α/(2π)×(1−4α/3) times Eq. (II.2). In these events there is no attempted recoil-induced emission associated with the stimulated emission. This is the reason for the factor of 1–4α/3. Part (e) shows events with a rate of α/(2π)×4α/3×[1−1/(2π)] times Eq. (II.2). These are sister events to those in (c), but where the attempted recoil-induced photon is not associated with an initial reabsorption, and has a probability of 1−1/(2π). Events (d) and (e) contribute to the anomalous magnetic moment and thus by the above introduced rule, the time-reversed stimulated emissions in (d) and (e), and the recoil-induced emission in (e) are suppressed, as denoted by the red crosses in Fig. VIII.3. Please notice that the five event rates displayed in Fig. VIII.3 sum to Eq. (II.2).

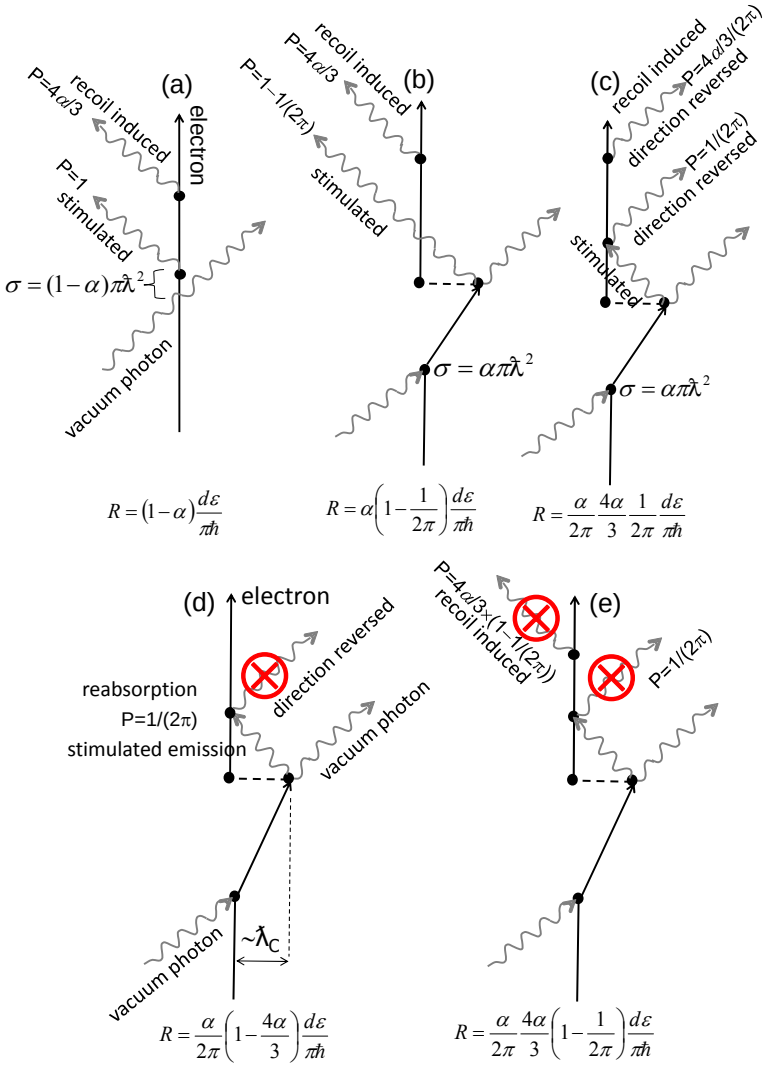

Fig. VIII.3. Five Feynman-like diagrams associated with recoil-induced emissions, and the anomalous magnetic moment of the electron (see text for details).

Event types (a), (b), and (c) give a virtual-photon emission rate of

$$R = \left(1-\frac{\alpha}{2\pi}\right)\left(1+\frac{4\alpha}{3}\right)+\frac{\alpha}{2\pi}\left(1+\frac{4\alpha}{3}\frac{1}{2\pi}\right)=1+\frac{4\alpha}{3}-\frac{2\alpha^2}{3\pi}\left(1-\frac{1}{2\pi}\right) \qquad \text{(VIII.2)}$$

The corresponding result for α is

$$\alpha = \frac{\left(1+\frac{4\alpha}{3}-\frac{2\alpha^2}{3\pi}\left(1-\frac{1}{2\pi}\right)\pm\alpha^3\right)^2}{139.7129683...}, \text{ which gives } \alpha = \frac{1}{137.0360(1)}, \qquad \text{(VIII.3)}$$

and a universal charge of q=1.602177(1)×10^{-19} C, consistent with experiment. The $\pm\alpha^3$ term is used to estimate a rough uncertainty associated with order-higher terms not considered here. Event types (d) and (e) give an anomalous magnetic moment of the electron

$$\frac{g-2}{2} = \frac{\alpha}{2\pi}\left(1-\frac{4\alpha}{3}\right)+\frac{\alpha}{2\pi}\frac{4\alpha}{3}\left(1-\frac{1}{2\pi}\right)=\frac{\alpha}{2\pi}\left(1-\frac{2\alpha}{3\pi}\pm\alpha^2\right)=0.00115961(6)\ , \qquad \text{(VIII.4)}$$

consistent with experiment. The $\pm\alpha^2$ term is used to estimate a rough uncertainty associated with higher-order- terms not considered here. The reader is reminded that Eq.s (VIII.3) and (VIII.4) are not based on first-principle expectations from a deep knowledge of QED but rather a plausibility argument in an attempt to rectify the discrepancy between Eq.s (VI.6) and (V.6), and the known experimental results. Without detailed calculations to justify the recoil-induced virtual emission, and the emission suppression associated with anomalous magnetic moment generating events, a healthy dose of skepticism should be applied.

IX. Summary and conclusions

By assuming that vacuum virtual photons can stimulate an isolated electron to emit additional virtual photons with a cross section of $\pi\lambda\!\!\!^{-2}$, and invoking a high-energy cutoff of $2\pi mc^2$ beyond which virtual photons no longer interact with a particle of mass m, the additional energy associated with the cloud of stimulated virtual photons surrounding a massless particle is on average equal to mc^2. This storage of the rest energy in the surrounding cloud of virtual photons is similar to the storage of the rest energy in the surrounding classical electric field, but without the infinity associated with point particles. A virtual-photon emission and self-absorption mechanism generates an inertia of $m=\varepsilon/c^2$. The high-energy cutoff of $2\pi mc^2$, in conjunction with the low-energy Lamb-shift cutoff suggested here, and an absorption/recoil/re-emission "doorway" cross section of $\alpha\pi\lambda\!\!\!^{-2}$, leads to a calculated hydrogen Lamb shift of 1058 MHz, in agreement with experiment. Additional support for a QED "doorway" cross section of $\alpha\pi\lambda\!\!\!^{-2}$ is obtained via a semi-classical picture of Compton scattering. The inclusion of semi-classical near-field effects and other model choices give the anomalous magnetic moment of the free electron. These choices are partially justified by their ability to also give an atomic number dependence of the magnetic moment of electrons in hydrogen-like atoms near the standard result obtainable via the Dirac equation.

An expression for the fine-structure constant can be obtained if electromagnetism is assumed to be associated with the exchange of stimulated virtual photons between particle pairs. Our first semi-classical estimate of the repulsive force obtained using only the far-field interaction cross section of $\pi\lambda\!\!\!^{-2}$, is infinite. Including an estimate of near-field effects and direction-reversing stimulated emission leads to a force that defines a fundamental unit of charge of $\sim 1.6\times10^{-19}$ C. The difference from the known value might be due to recoil effects, perhaps as speculated in section VIII. By including these effects, an inverse fine-structure constant of $\alpha^{-1}=137.0360(1)$ and a corresponding calculated universal charge of $1.602177(1)\times10^{-19}$ C are obtained, along with an anomalous magnetic moment of $(g-2)/2 = 0.00115961(6)$. The direction-reversing stimulated-emission process used to give a favorable result for α, suggests a Larmor emission mechanism that gives an emission power close to the corresponding classical result. Conservation of energy can be maintained in Larmor emissions without invoking the electromagnetic force of an electron on itself. We feel that we cannot currently dismiss the possibility that the fine-structure constant and several other QED results are obtainable via a far-field emission/absorption cross section of $\pi\lambda\!\!\!^{-2}$ with near-field effects, direction-reversing stimulated emission, and recoil corrections. A summary of our reverse-engineered semi-classical results is presented in Table IX.1 and Fig. IX.1.

Additional work on photon-particle near-field corrections, direction-reversing stimulated emission, and recoil effects is needed to confirm or negate the semi-classical shenanigans performed here. If the semi-classical choices made here can be justified by detailed calculations, then an understanding of the numerical value of the fine-structure constant may emerge. Despite the speculative nature of several of the arguments used to obtain a calculated value near to the known fine-structure constant, the present

study suggests that charge is an emergent property generated by a simple interaction mechanism between point-like particles and the electromagnetic vacuum, similar to the mechanisms that generate the Lamb shift and the anomalous magnetic moment of the electron.

Table IX.1. Summary of the semi-classical results obtained here, and a comparison with QED.

Observable	Simple reverse-engineered results		QED
	Reason	Formula	
Rest energy	Emission and self-absorption of stimulated virtual photons	$E = \int_0^{2\pi mc^2} \int_0^{\infty} \frac{2\varepsilon^2}{\pi\hbar^2} t \exp(-2\varepsilon t/\hbar)\, dt\, d\varepsilon = mc^2$	
Inertia	Doppler shift of the returning self-absorbed virtual photons	$F = \frac{1}{2\pi\hbar c} \int_0^{\pi} \int_0^{2\pi mc^2} \left(\frac{3a\hbar}{2c} \cos^2(\theta) \sin(\theta)\right) d\varepsilon\, d\theta = ma$	N/A
Lamb shift (excluding vacuum polarization and the shift of the p state)	Absorption and re-emission of vacuum virtual photons	$\Delta E_{2s} = \frac{\alpha^5 \ln(2\pi^2/\alpha)}{6\pi} mc^2 = 1072$ MHz	1072 MHz
Compton scattering	Absorption, recoil, and re-emission of the incident photon	$\sigma = \alpha\pi\lambda^2 \frac{4\alpha}{3} \frac{\varepsilon^2}{(mc^2)^2} 2 = 8\pi(\alpha\lambda_C)^2/3$	$8\pi(\alpha\lambda_C)^2/3$
Anomalous magnetic moment of the free electron	Stimulated emission and reabsorption including near-field and recoil effects, following the absorption and re-emission of vacuum virtual photons	$\frac{(g-2)}{2} = \frac{\alpha}{2\pi}\left(1 - \frac{4\alpha}{3}\frac{1}{2\pi}\right)$ =0.00115961	$\frac{\alpha}{2\pi}\left(1 - 0.985 \ldots \frac{4\alpha}{3}\frac{1}{2\pi}\right)$ 0.0011596522 (experiment)
Magnetic moment of the electron in hydrogen-like atoms	Stimulated emission and reabsorption including near-field effects and system size	$g(1s) = g_e(1 - \frac{\pi}{3}\frac{\alpha^2 Z^2}{3})$	$g_e(1 - \frac{\alpha^2 Z^2}{3})$
Fine-structure constant	Exchange of stimulated virtual photons including near-field, direction-reversing, and recoil effects	$\alpha = \frac{(1 + 4\alpha/3 - 2\alpha^2/(3\pi))^2}{2\pi} \int_0^{2\pi} \frac{\mathrm{erf}^4(\varepsilon/2^{3/2})}{\varepsilon\,[\exp(\varepsilon) - 1]} d\varepsilon$ α=1/137.0360	1/137.0359991 (experiment)
Larmor formula	Scattering of direction-reversed stimulated emission	$P = \frac{2}{\pi} \int_0^{2\pi} \frac{\mathrm{erf}^4(\varepsilon/2^{3/2}) \exp(-\varepsilon)}{\varepsilon\,[\exp(\varepsilon) - 1]} d\varepsilon\, a^2 \frac{\hbar}{c^2}$ =1.016 ... $\frac{2}{3}\alpha a^2 \frac{\hbar}{c^2}$	$\frac{2}{3}\alpha a^2 \frac{\hbar}{c^2}$

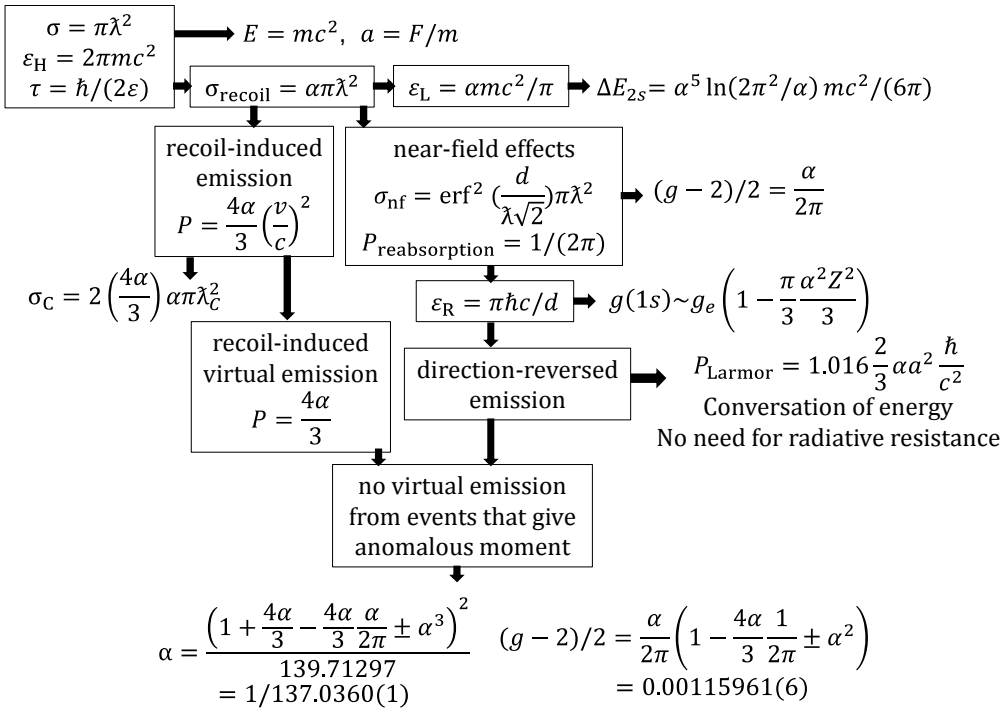

Fig. IX.2. Summary of the connection between assumptions (rectangles) and results.

References

[AOY07] T. Aoyama, M. Hayakawa, T. Kinoshita, and M. Nio, Phys. Rev. Lett. **99**, 110406 (2007).

[AOY12] T. Aoyama, M. Hayakawa, T. Kinoshita, and M. Nio, Phys. Rev. D **85**, 033007 (2012).

[BEK77] J. D. Bekenstein and A. Meisels, Phys. Rev. **D 15**, 2775 (1977).

[BET47] H. A. Bethe, Phys. Rev. **72**, 339 (1947).

[BET50] H. A. Bethe, L. M. Brown, and J. R. Stehn, Phys. Rev. **77**, 370 (1950).

[BJO64] J. D. Bjorken and S. D. Drell, Relativistic Quantum Mechanics, McGraw-Hill ISBN 07-005493-2 (1964).

[DIR27] P. A. M. Dirac, Proc. Roy. Soc. (London) **A114**, 243 (1927), **A117**, 610 (1928).

[DYS49] F. Dyson, Phys. Rev. **75**, 486 (1949), **75**, 1736 (1949).

[FEY49] R. P. Feynman, Phys. Rev. **76**, 749 (1949), **76**, 769 (1949).

[FEY62] R. P. Feynman, R. B. Leighton, and M. Sand, The Feynman Lecture on Physics, Definitive Edition, Vol II, section 28-4, Pearson Addison and Wesley (2006).

[GAB06] G. Gabrielse, D. Hanneke, T. Kinoshita, M. Nio, and B. Odom, Phys. Rev. Lett. **97**, 030802 (2006) and **99**, 039902 (2007).

[GRO70] H. Grotch, Phys. Rev. Lett. **24**, 39 (1970).

[HAN56] R. Hanbury Brown and R. Q. Twiss, Nature **177**, 27 (1956), and R. Hanbury Brown and R. Q. Twiss, Nature **178**, 1046 (1956).

[IRA08] Z. Irahharten et al., IEEE International Conference on Communication, 2008, pg. 4872.

[JAC75] J. D. Jackson, Classical Electrodynamics, John Wiley & Sons, Inc. (1975).

[KAR52] R. Karplus, A. Klein, and J. Schwinger, Phys. Rev. **86**, 288 (1952).

[KAR98] S. G. Karshenboim, Can. J. Phys. **76**, 168 (1998).

[KEM33] E. C. Kemble and R. D. Present, Phys. Rev. **44**, 1031 (1933).

[KIN06] T. Kinoshita and M. Nio, Phys. Rev. D **73**, 013003 (2006).

[LAM47] W. E. Lamb and R. C. Retherford, Phys. Rev. **72**, 241 (1947).

[LAP96] S. Laporta and E. Remiddi, Phys. Lett. B, **379**, 283 (1996).

[LES08] J. P. Lestone, Mod. Phys. Lett. A, **23**, 1067 (2008).

[MOH15] P. J. Mohr et al, http:/physics.nist.gov/constants (2015), National Institute of Standards and Technology, Gaithersburg, MD 20899, USA.

[PET57] A. Petermann, Helv. Phys. Acta, **30**, 407 (1957).

[SCH48] J. Schwinger, Phys. Rev. **73**, 416 (1948), **74**, 1439 (1949), **76**, 790 (1949).

[TIE77] J. S. Tiedeman and H. G. Robinson, Phys. Rev. Lett. **39**, 602 (1977).

[TOM46] S. Tomonaga, Prog. Theor. Phys. **1**, 27 (1946).

[UEH35] E. A. Uehling, Phys. Rev. **48**, 55 (1935).

[WEL48] T. A. Welton, Phys. Rev. **74**, 1157 (1948).